Organization of Organic Molecules with Inorganic Molecular Species into Nanocomposite Biphase Arrays†

Qisheng Huo,‡ David I. Margolese,‡ Ulrike Ciesla,§ Dirk G. Demuth,§ Pingyun Feng,‡ Thurman E. Gier,‡ Peter Sieger,‡ Ali Firouzi,⊥ Bradley F. Chmelka,⊥ Ferdi Schüth,§ and Galen D. Stucky*,‡

Department of Chemistry, University of California, Santa Barbara, California 93106; Institut für Anorganische Chemie, Johannes Gutenberg-Universität, 55099 Mainz, Germany; and Department of Chemical and Nuclear Engineering, University of California, Santa Barbara, California 93106

Received February 8, 1994. Revised Manuscript Received June 14, 1994®

The organization of cationic or anionic organic and inorganic molecular species to produce three-dimensional periodic biphase arrays is described. The approach uses cooperative nucleation of molecular inorganic solution species with surfactant molecules and their assembly at low temperatures into liquid-crystal-like arrays. The organic/inorganic interface chemistry makes use of four synthesis routes with (S^+I^-), (S^-I^+), ($S^+X^-I^+$), and ($S^-M^+I^-$) direct and mediated combinations of surfactant (cationic S^+, anionic S^-) and soluble inorganic (cationic I^+, anionic I^-) molecular species. The concepts can be widely applied to generate inorganic oxide, phosphate or sulfide framework compositions. Distinct lamellar, cubic silica mesophases were synthesized in a concentrated acidic medium ($S^+X^-I^+$), with the hexagonal and the cubic phases showing good thermal stability. For the hexagonal mesostructured silica materials high BET surface areas (>1000 m^2/g) are found. Hexagonal tungsten(VI) oxide materials were prepared in the presence of quaternary ammonium surfactants in the pH range 4–8. Cubic (*Ia3d*) and hexagonal antimony(V) oxides were obtained by acidifying (pH = 6–7) homogeneous solutions of soluble Sb(V) anions and quaternary ammonium surfactants at room temperature (S^+I^-). Using anionic surfactants, hexagonal and lamellar lead oxide mesostructures were found (S^-I^+). Crystalline zinc phosphate lamellar phases were obtained at low synthesis temperatures (4 °C) and lamellar sulfide phases could be also readily generated at room temperature. The synthesis procedure presented is relevant to the coorganization of organic and inorganic phases in biomineralization processes, and some of the biomimetic implications are discussed.

Introduction

Margaret Etter led chemists to the realization of being able to put together collections of organic molecules in a preferred way, using the idiosyncrasies of each molecular species to define it as a building block in the formation of an extended solid-state structure with predesigned properties: "Take a single organic molecule and learn how it hydrogen-bonds to different kinds of molecules..., then put it into a solid and surround it with molecules different from itself."[1]

In this paper we extend the self-organization concepts of Margaret Etter to the synthesis[2,3] of organic/inorganic biphase materials by tailoring molecular metal-ion speciation and charge density to control organic array assembly at the inorganic/organic interface.

Much of the interest, beauty and potential in this field comes from the incentive provided by the many intricate, architecturally exquisite, and structurally robust examples of organic/inorganic biphase structures that exist in nature. The central tenet of mimicking biomineralization emphasizes that nucleation, growth, final morphology and overall aggregation of inorganic species are determined by organized assemblies of organic macromolecules.[4-7] As a consequence, biomimetic approaches and modeling of biomineralization have for all practical purposes relied exclusively on this paradigm for experimental design. The approach presumes first the existence or construction of an organized organic surface which controls the subsequent nucleation of the inorganic species by geometric, electrostatic and/or stereochemical interactions between inorganic nuclei and the functionalized substrate. Recent developments in this area include (i) the synthesis of layered siloxane networks using self-assembled bilayers formed from amphiphiles,[8,9] (ii) hollow submicron-diameter silica cylinders obtained by depositing silica onto phospholipid tubules,[10] (iii) silica polymers generated in

† In memory of Professor Margaret Etter.
‡ Department of Chemistry, University of California.
§ Johannes Gutenberg-Universität.
⊥ Department of Chemical and Nuclear Engineering, University of California.
* Author for correspondence.
® Abstract published in *Advance ACS Abstracts*, August 15, 1994.

(1) Etter, M. C. *The Washington Post*, **1989**, Sunday, August 20, B3.
(2) Monnier, A.; Schüth, F.; Huo, Q.; Kumar, D.; Margolese, D.; Maxwell, R. S.; Stucky, G. D.; Krishnamurty, M.; Petroff, P.; Firouzi, A.; Janicke, M.; Chmelka, B. F. *Science*, **1993**, *261*, 1299.
(3) Stucky, G. D.; Monnier, A.; Schüth, F.; Huo, Q.; Kumar, D.; Margolese, D.; Krishnamurty, M.; Petroff, P.; Firouzi, A.; Janicke, M.; Chmelka, B. F. *Mol. Cryst. Liq. Cryst.* **1994**, *240*, 187.
(4) Weiner, S. *Crit. Rev. Biochem.* **1986**, *20*, 365.
(5) Mann, S. *Nature* **1988**, *332*, 119.
(6) Mann, S.; et al. *Science* **1993**, *261*, 1286.
(7) Mann, S. *Nature* **1993**, *365*, 499.
(8) Sakata, K.; Kunitake, T. *Chem. Lett.* **1989**, 2159.
(9) Sakata, K.; Kunitake, T. *J. Chem. Soc., Chem. Commun.* **1990**, 504.
(10) Baral, S.; Schoen, P. *Chem. Mater.* **1993**, *5*, 145.

0897-4756/94/2806-1176$04.50/0

a lamellar mesophase consisting of didodecyldimethylammonium bromide and water,[11] (iv) iron oxide deposited organic tubules with bulk inorganic phases grown on charged biolipid substrate,[12] and (v) ceramic thin-film processing by deposition of bulk inorganic phases on surfaces functionalized with ionic organic surfactants.[13]

There is no doubt that stable organized organic arrays can be an important part of inorganic nucleation and phase formation in biosystems. However, a biomimetic model which neglects the possibility and use of mutually induced structural modifications of the organic and inorganic phases makes it difficult to design synthetically beyond the condensation of bulk inorganic phases onto stabilized charged organic surfaces or to create biomimetically biphases with higher order complex microstructures which, as in nature, can contain as little as 1 wt % organic homogeneously assembled with the remaining 99% inorganic phase. A more general biomimetic approach is needed which takes into account the dynamic balance between organic array assembly, inorganic polymerization, and the necessary interface chemistry.

Mobil scientists' success in the synthesis of mesoporous molecular sieves (M41S), of which MCM-41 (hexagonal) and MCM-48 (cubic) are two typical members, is a major breakthrough in the synthesis of organic/inorganic biphase composite materials.[14,15] For the first time the one-step syntheses of distinct coarrays of cationic organic molecules and anionic inorganic polymeric phases in a variety of periodic mesostructural composite configurations were demonstrated. However, at first glance the central theme of biomimetics would appear to apply for these materials as well: first create an organized organic array, and then condense an inorganic phase on the preorganized organic surface.[16,17]

In this paper we emphasize the application of an alternative approach to biphase-array synthesis, based on the cooperative formation of inorganic-organic interfaces[3,18,47] in which the multidentate charge density of soluble *molecular* inorganic species determines the initial organic molecular siting and array possibilities. The hydrophobic portions of the organic phase then organize within this "charge density matching" constraint in a cooperative fashion, minimizing the organic van der Waals, inorganic and organic charge energies to form the resulting mesostructure. This is a dynamic model which does not require the existence of preorganized organic arrays, and, if they are present, the cooperative formation of the inorganic–organic interface can be expected to create new organic array configurations. This model is applied to a variety of surfactant and inorganic phase precursors to construct three dimensional biphase arrays. In contrast to the usual biomimetic approach (e.g., i–v above) this strategy goes beyond the deposition of bulk inorganic phases on a charged organic substrate surface and instead uses one-step syntheses to create 3-d organized biphase arrays for a variety of positively and negatively charged inorganic compositions and classes of surfactants.

We have indicated previously that these concepts might be applied to the synthesis of transition metal oxide mesostructures[2] and reported in a preliminary note the synthesis of both transition and main-group metal mesostructure materials.[19] Such materials offer the possibility of forming nanocomposite electrochromic or solid electrolyte devices[20,21] as well as high surface area redox active catalyst[22] and bioseparation substrates.

An alternative approach to biomimetics is to use such a coorganization of organic and inorganic phases in biomineralization processing.[7] However, in contrast to the M41S family, organic bioarrays are generally based on anionic (e.g., carboxylate, phosphate, and sulfate) groups and their implied interaction with cationic inorganic phases. Mimicking such processes to synthesize biorelevant composite phases with intricate microstructural assemblies using anionic as well as cationic organic phases is therefore an important goal.

Here we describe the synthesis of mesophases (including transition-metal oxide mesophases) with cationic and anionic surfactants and soluble inorganic species using variable pH conditions. This inorganic–organic assembly mechanism is shown to apply to a variety of solidification processes by using low temperature techniques[23] with surfactant or lipid arrays through the cooperative assembly of molecular inorganic species. This includes the formation of organized periodic porous silica at room temperature in concentrated acid solution (1–7 mol L^{-1} HCl:H_0 = 0 to −2.5).

Experimental Section

Chemicals. The following surfactants were used in the synthesis: (i) cationic surfactants, exclusively quaternary alkylammonium salts, such as $C_nH_{2n+1}(CH_3)_3NBr$ (C_nTMABr, n = 8, 10, 12, 14, 16, 18), commercially available from Aldrich Chemical Co. Inc., and $C_nH_{2n+1}(CH_3)_3NBr$ (n = 20, 22) or the dimeric surfactants $[C_mH_{2m+1}(CH_3)_2N–C_sH_{2s}–N(CH_3)_2C_mH_{2m+1}]Br_2$ (m = 16, s = 2–12) synthesized and purified as described in refs 24 and 25, respectively; (ii) anionic surfactants, namely phosphates ($C_{12}H_{25}OPO_3H_2$), sulfates ($C_nH_{2n+1}OSO_3Na$, n = 12, 14, 16, 18), sulfonates ($C_{16}H_{33}SO_3H$ and $C_{12}H_{25}C_6H_4SO_3Na$) and carboxylic acids (for example stearic acid $C_{17}H_{35}CO_2H$), also commercially available from Aldrich, Lancaster or Fisher. Sodium silicate solution N was purchased from PQ corporation. Other inorganic materials were $Si(OC_2H_5)_4$ (TEOS) and water soluble materials like $Zn(NO_3)_2$, H_3PO_4, $K[Sb(OH)_6]$, $(NH_4)_6H_2W_{12}O_{40}$, $SnCl_4·5H_2O$, $Na_2S·9H_2O$, $MnCl_2·6H_2O$, $FeCl_2·4H_2O$, $FeCl_3·6H_2O$ $Ni(NO_3)_2·6H_2O$, $Co(NO_3)_2·6H_2O$, $Pb(NO_3)_2$, $Al(NO_3)_3$ and for varying the pH

(11) Dubois, M.; Gulik-Krzywicki, T.; Cabane, B. *Langmuir* **1993**, *9*, 673.
(12) Archibald, D. D.; Mann, S. *Nature* **1993**, *364*, 430.
(13) Bunker, B. C.; Rieke, P. C.; Tarasevich, B. J.; Campbell, A. A.; Fryxell, G. E.; Graff, G. L.; Song, L.; Liu, J.; Virden, J. W.; McVay, G. L. *Science* **1994**, *264*, 48.
(14) Kresge, C. T.; Leonowicz, M. E.; Roth, W. J.; Vartuli, J. C.; Beck, J. S. *Nature* **1992**, *359*, 710.
(15) Beck, J. S.; Vartuli, J. C.; Roth, W. J.; Leonowicz, M. E.; Kresge, C. T.; Schmitt, K. T.; Chu, C. T.-W.; Olson, D. H.; Sheppard, E. W.; McCullen, S. B.; Higgins, J. B.; Schlenker, J. L. *J. Am. Chem. Soc.* **1992**, *114*, 10834.
(16) Chen, C.; Li, H.; Davis, M. E. *Microporous Mater.* **1993**, *2*, 17.
(17) Chen, C.; Burkett, S. L.; Li, H.; Davis, M. E. *Microporous Mater.* **1993**, *2*, 27.
(18) Chmelka, B. F.; Firouzi, A.; Oertli, A.; Kumar, D.; Huo, Q.; Walker, S. J.; Zasadzinski, J. A.; Glinka, C.; Nicol, J.; Rush, J.; Margolese, D.; Stucky, G. D., submitted to *Science*.
(19) Huo, Q.; Margolese, D. I.; Feng, P.; Gier, T. E.; Sieger, P.; Stucky, G. D.; Leon, R.; Petroff, P.; Ciesla, U.; Schüth, F. *Nature* **1994**, *368*, 317.
(20) Lampert, C. M.; Granqvist, C. G. *Large-Area Chromogenics: Materials and Devices for Transmittance Control*; Lampert, C. M., Granqvist, C. G., Eds.; SPIE Optical Engineering Press: Washington, 1990; p 2.
(21) Dautremont-Smith, W. C. *Displays* **1982**, *3*, 3.
(22) Parton, R. F.; Jacobs, J. M.; van Ooteghem, H.; Jacobs, P. A. *Zeolites as Catalysts, Sorbents and Detergent Builders*; Karge, H. G., Weitkamp, J., Eds.; Elsevier Science Publishers: Amsterdam, 1989; p 211.
(23) Gier, T. E.; Stucky, G. D. *Nature* **1991**, *349*, 508.
(24) Bacaloglu, R.; Bunton, C. A.; Ortega, F. *J. Phys. Chem.* **1989**, *93*, 1497.
(25) Zana, R.; Benrraou, M.; Rueff, R. *Langmuir* **1991**, *7*, 1072.

normally aqueous solutions of HCl, HBr, NH_3, NaOH, and $(CH_3)_4NOH$ were taken.

Synthesis. Following are some typical synthesis examples.

I. S^+I^- = Cationic Surfactant S^+/Soluble Anionic Inorganic Species I^-. *Tungsten oxide*: The tungsten oxide–surfactant samples were prepared as follows: A solution of 30 g of 25 wt% $C_nH_{2n+1}(CH_3)_3NBr$ with n = 12, 14, 16, 18 (in the case of hexadecyl surfactant the chloride compound was used) was combined with a solution contaning 3 g (1.01 mmol) of ammonium metatungstate ($(NH_4)_6H_2W_{12}O_{40}$) and 30 g of H_2O. The pH of this solution was adjusted by addition of aqueous NH_3 or aqueous HCl. The mixture was stirred for 30 min and then heated at 90 °C for 3 days. After cooling to room temperature the solid white product was recovered by filtration, washed with water, and air-dried.

Antimony oxide: Precipitation of antimony oxide mesostructured materials was performed by acidifying homogeneous solutions of $K[Sb(OH)_6]$ and surfactant at room temperature. A typical example is as follows: 1.31 g (5 mmol) of $K[Sb(OH)_6]$ and (i) 0.182 g (0.5 mmol) and (ii) 0.364 g (1 mmol) of $C_{18}H_{37}(CH_3)_3NBr$ were dissolved in 50 g of H_2O by heating the mixture to the boiling point. The clear homogeneous and cooled solutions of pH = 7.0 were then acidified by adding dropwise an aqueous 0.1 mol L^{-1} HBr solution under pH control forming immediately a white precipitate. After one night at room temperature the precipitates were separated from the mixtures by filtering then washed carefully with water and finally dried at room temperature.

Tin sulfide: A tin sulfide lamellar phase was synthesized by using $C_{16}H_{33}(CH_3)_3NBr$ as template at room temperature for 3 days. Typical reaction mixture composition is as follows: 0.87 g of $Na_2S{\cdot}9H_2O$, 0.31 g of $C_{16}H_{33}(CH_3)_3NBr$, 1.0 g of $SnCl_4{\cdot}5H_2O$, 6 g of 2 mol L^{-1} NaOH solution, and 26 g of H_2O.

II. S^-I^+ = Anionic Surfactant S^-/Soluble Cationic Inorganic Species I^+. *Fe^{2+} and Pb^{2+} with alkyl sulfonates*: The synthesis of the Pb oxide surfactant compound was carried out as follows: A solution of 3.5 g (10.6 mmol) of $Pb(NO_3)_2$ in 20 g of H_2O was adjusted to pH 7–8 by addition of 0.1 mol L^{-1} NaOH. This solution was combined with a suspension containing 0.55 g (1.67 mmol) of $C_{16}H_{33}SO_3Na$ in 20 g of H_2O and stirred for 30 min. The mixture was heated at 90 °C for 3 days. The product was filtered, washed with water and air-dried. The synthesis procedure for the Fe oxide surfactant differed: A freshly prepared solution of 2.0 g (10 mmol) of $FeCl_2{\cdot}4H_2O$ with a pH of 3 was added to a surfactant suspension of 1.0 g (3.04 mmol) $C_{16}H_{33}SO_3Na$ in 25 g of H_2O. At this point the pH was adjusted to 6 by adding aqueous NH_3. After standing for 2 days at room temperature, the brown yellow product was filtered, washed with water and air-dried.

Mg^{2+}, Al^3, Mn^{2+}, Ga^{3+}, Fe^{3+}, Co^{2+}, Ni^{2+}, and Zn^{2+} with alkyl phosphates: The synthesis using Mg^{2+} and Zn^{2+} as typical examples are described as follows: (i) A small polypropylene bottle was filled with 1.598 g (6 mmol) of $C_{12}H_{25}OPO_3H_2$, 30 g of H_2O, and 2.87 g (10 mmol) of a 4 mol L^{-1} NaOH solution forming a clear solution after stirring. A 2 mol L^{-1} (3.00 g, 5 mmol) $Mg(NO_3)_2$ solution was then added, forming a gel which aggregated on shaking (pH = 4.5). After being held for 13 days at 100 °C, the powder was recovered by standard filtration technique and found to have a layer spacing of 30.9 Å. (ii) Another polypropylene bottle was charged with 1.598 g (6 mmol) of $C_{12}H_{25}OPO_3H_2$, 30 g of H_2O, and 2.87 g (10 mmol) of a 4 mol L^{-1} NaOH solution forming again a clear solution to which 3.217 g (5 mmol) of a 2 mol L^{-1} $Zn(NO_3)_2$ solution was added to give a white rapidly settling precipitate (pH = 3). After holding the reaction for 5 days at 100 °C, the solid was recovered by standard vacuum filtration.

Fe^{2+}, Fe^{3+}, Ni^{2+}, Co^{2+}, and Mn^{2+} with alkyl sulfates: A representative example for this kind of combination can be described as follows: 0.172 g (0.5 mmol) of $C_{16}H_{33}OSO_3Na$, dissolved in 10 mL of H_2O, was slowly dropped into 50 mL of a freshly prepared 0.1 mol L^{-1} $FeCl_2{\cdot}4H_2O$ (pH = 2.8) solution. After adding about half of the amount of surfactant precipitation of a yellow solid material occurred. After standing over night at room temperature the solid product was separated by filtration, washed carefully with water, and finally air-dried.

III. $S^+X^-I^+$ = Cationic Surfactant S^+/Intermediate Anion X^-/Soluble Cationic Inorganic Species I^+. *Silica mesophases*: Generally each of the three acid silica structural phases (lamellar, hexagonal or *Pm3n* cubic) was prepared as follows: first, quaternary ammonium surfactant was mixed with water and HCl or HBr. To this solution tetraethyl-orthosilicate (TEOS) was added at room temperature and stirred for 30 min or longer. The solid product was recovered by filtration and dried at room temperature.

Zinc phosphate: The products were obtained by crystallization of a sol of zinc phosphate containing surfactant. A typical example is described as follows: A polypropylene bottle was charged with 1.93 g (3 mmol) of 2 M $Zn(NO_3)_2$, 1.048 g (3.5 mmol) of 4 M H_3PO_4, 1.82 g (5 mmol) of $C_{16}H_{33}(CH_3)_3NBr$, and 14 g of water. After mild warming, a clear syrupy solution resulted, and 1.64 g (4.5 mmol) of 25% aqueous $(CH_3)_4NOH$ (tetramethylammonium hydroxide) was added to give a sol. The reaction mixture (pH = 2) was stored at 4 °C for 18 days and then recovered using standard filtration, washing and air drying techniques.

IV. $S^-M^+I^-$ = Anionic Surfactant S^-/Intermediate Cation M^+/Soluble Anionic Inorganic Species I^-. *Al^{3+} with alkyl phosphate*: A small polypropylene bottle (60 mL) was charged with 1.465 g (5.5 mmol) of $C_{12}H_{25}OPO_3H_2$, 30 g of H_2O, and 4.31 g (15 mmol) of a 4 mol L^{-1} NaOH solution. The mixture was warmed to give a clear solution and 3.27 g (5 mmol) of 2 mol L^{-1} $Al(NO_3)_3$ solution was added. The initial gel transformed rapidly to a white milk. The material was sealed at 100 °C for 10 days, and the white hydrophobic solid was recovered by standard vacuum filtration (pH = 5). This synthesis was repeated using only 15 g of H_2O and 5.74 g (20 mmol) of a 4 mol L^{-1} NaOH solution resulting in a final pH = 8 after 10 days at 100 °C. The product is also a hydrophobic powder.

Analysis. X-ray powder diffraction patterns were taken on a Scintag PADX diffractometer equipped with a liquid nitrogen cooled germanium solid-state detector using Cu Kα radiation. The low-angle synchrotron X-ray diffraction pattern shown in Figure 10c of the cubic (*Pm3n*) siliceous mesophase was measured at Brookhaven National Laboratory. A Ge(111) incident beam monochromator and a Ge(220) analyzer crystal were used to obtain a monochromatic wavelength of λ = 1.7048 Å. High-resolution ^{27}Al, ^{29}Si, and ^{31}P MAS NMR spectra were recorded on a GE 300 spectrometer using 7-mm ZrO_2 rotors. Single-pulse excitation was applied in combination with high-power proton decoupling. Measurement conditions were as follows: ^{27}Al resonance frequency, 78.170 MHz; pulse repetition, 0.1 s; pulse width, 0.7 μs, spinning speed 5–6 kHz, standard, $Al(NO_3)_3$ solution. ^{29}Si resonance frequency, 59.705 MHz; pulse repetition, 240 s; pulse width, 7 μs; spinning speed, 5–6 kHz, standard, $(CH_3)_4Si$. ^{31}P resonance frequency, 121.66 MHz; pulse repetition, 20 s; pulse width, 7 μs; spinning speed, 5–6 kHz, standard, 85% H_3PO_4. The usual notation Q^x will be used for the Si sites, where x refers to the number of Si surrounding the central Si atom bridged by oxygen atoms. A Netzsch Thermoanalyzer STA 409 was used for simultaneous thermal analysis (STA) combining thermogravimetry (TG), derivative thermogravity (DTG), and difference thermoanalysis (DTA) with heating rates of 2 K min^{-1} in air. Elemental analyses were performed by Galbraith Laboratories (Knoxville, TN). BET measurements were performed by Micromeritics (Norcross, GA).

Results and Discussion

Synthesis Model. The synthesis involves the organization of hydrophobic and hydrophilic entities into a homogeneous biphase composite. In view of the well-defined spatial separation of the organic/inorganic phases within the product phases, three types of nearest-neighbor assembly are evident: inorganic–organic, organic–organic, and inorganic–inorganic. For these reasons we therefore consider the free energy and kinetics of formation of the mesostructure in terms of the relative contributions of (i) formation of the interface of the inorganic/organic phases, (ii) organization of the organic array, (iii) interactions between inorganic units, including polymerization and

hydrogen bonding, and (iv) the chemical potential of the surrounding solution phase during synthesis. In this context the free energy terms can be summarized as

$$\Delta G = \Delta G_{inter}(A,\rho_{inorg},\rho_{org},...) + \Delta G_{org}(A,\rho_{org},...) + \Delta G_{inorg}(\rho_{inorg},...) + \Delta G_{sol} \quad (1)$$

In this research amphiphilic organic groups were used with hydrophobic tails and ionic head groups. For these organics, A is the effective area occupied by the ionic surfactant head group in the organic phase (e.g., the $(CH_3)_3N^+$ group in $[C_nH_{2n+1}(CH_3)_3N]^+X^-$ (C_nTMAX) surfactants). The optimal head-group area, A_0, is obtained by minimizing the free energy change, ΔG, i.e., $A_0 \rightarrow (\partial \Delta G/\partial A) = 0$). ρ is a generic variable representing the state of the phase by specifying the organization and charge distribution of the various species within it. $1/A$ is a measure of the average organic surface charge density. Experimentally it is observed and readily modeled that for a given surfactant a curved organic array surface has a substantially lower charge density at equilibrium than a flat surface (A_{min} = 70 Å^2, 46.7 Å^2, and 23.3 Å^2 for spherical, rodlike, and lamellar C_{12}TMABr, respectively, at room temperature).[26a] The critical role of the effective head-group area in determining the energetics of surface curvature and the type of biphase surfactant structure formed is extensively documented[26] and can be expected to be as important in matching inorganic molecular species such as silicate anions as it is with more simple inorganic ions such as Cl^- or OH^-. A is therefore an obviously important parameter when electrostatic ion pairing between surfactant and counterion is energetically dominating. The interface wall charge and thickness are defined by ρ. For pure aqueous surfactant phases the interface wall thickness is also a function of the cation–cation repulsion due to the cationic charge densities ($\propto 1/A$) and the cation–anion/solvent interactions.

$\Delta G_{org}(A,\rho_{org},...)$ results from the van der Waals forces and conformational energy of the hydrocarbon chains and the van der Waals and electrostatic interactions of the head groups within the organic subphase. It is related to the free energy of micellization for ionic surfactants defined by Evans et al.[27] which can be expressed as ΔG(micellization) = $\Delta g_{el} + \gamma A + \Delta g$(HP) where Δg_{el} is the free energy associated with assembling a double layer, γ is the surface tension of the micelle water interface, and Δg(HP) is the free energy of transferring the hydrocarbon chain out of water and into the oil-like interior of the micelle. The role of the anion and the anion–cation interface free energy contributions are not explicitly addressed in this description but are implicitly included. In this sense ΔG and $\Delta G_{org}(A,\rho_{org},...)$ differ from ΔG(micellization).

$\Delta G_{inorg}(\rho_{inorg},...)$ reflects the contributions arising from the inorganic subphase. If the inorganic phase consists of unpolymerized inorganic molecular species, it describes the energetics of the charge and inorganic intermolecular interactions. This is also a measure of the polymerized inorganic phase (e.g., polysilicate) structural free energy, including the solvent, van der Waals, and electrostatic interactions within the inorganic framework or "wall" if they are present.

$\Delta G_{inter}(A,\rho_{inorg},\rho_{org},...)$ accounts for the van der Waals and electrostatic effects associated with inorganic/organic array interactions. ΔG_{sol} represents the contribution of the mother liquor solution. This contribution sets the chemical potential of the various species during nucleation and within the precipitate.

The biomimetic approaches described above,[8-12] which start with an organized organic array and carry out inorganic growth on its surface, is a statement that the most important free energy and/or kinetic contribution to biphase composite formation is the organization of the organic array. The free energy changes associated with the interface between the inorganic and organic phases, and the organization/condensation of the inorganic phase are regarded as perturbations on the organized array, i.e.

$$\Delta G_{org}(A,\rho_{org},...) < \Delta G_{inter}(A,\rho_{inorg},\rho_{org},...) < \Delta G_{inorg}(\rho_{inorg},...) \quad (2)$$

This is also the model proposed by Chen and Davis et al.[16,17,49] for the formation of the MCM-41 and MCM-48 phases. The observation of a single isotropic line in the ^{14}N NMR spectra of gels during the *in situ* synthesis of MCM-41 and MCM-48 is assigned to the presence of rapidly rotating rodlike micelles which are subsequently coated with silicate species. In this model it is suggested that the starting point for the synthesis mechanism for the M41S phases requires that the C_{16}TMA cations are organized into rodlike micelles.

The cooperative "templating" perspective for the mechanism of formation of the MCM-41 and MCM-48 silicate phases is that the electrostatic interface interaction between soluble anionic inorganic molecular species and cationic monotailed surfactant molecules is responsible for initiating the composite synthesis and that the preorganized organic array is not necessary, or if present not necessarily related to the morphology of the final composite product[3,19] (Figure 1). This point of view, which is supported by *in situ* measurements,[18] argues that at the very least the kinetics of low-temperature syntheses of periodic mesocomposite are better described by

$$k_{inter}(A,\rho_{inorg},\rho_{org},...) > k_{org}(A,\rho_{org},...) > k_{inorg}(\rho_{inorg},...) \quad (3)$$

where k_{inter}, k_{org}, and k_{inorg} are respectively the relative rates for cation–anion formation, the organic array assembly as it exists in the final mesostructure configuration and silica polymerization. This model also states that for monotailed surfactant/polydentate (polycharged) inorganic ion combinations

$$\Delta G_{inter}(A,\rho_{inorg},\rho_{org},...) < \Delta G_{org}(A,\rho_{org},...) \quad (4)$$

All terms in eq 1 are important so that the particular approach to biomimetics and nanocomposite structure synthesis can be varied by changing organic and inorganic interactive forces, temperature, and concentration (i.e., lyotropic parameters). For example van der Waals forces and organic array stability are greater for bitailed surfactants than for monotailed surfactants so that $\Delta G_{org}(A,\rho_{org},...)$ becomes a more important contribution.

(26) See for example: (a) Bleasdale, T. A.; Tiddy, G. J. T. In *The Structure, Dynamics and Equilibrium Properties of Colloidal Systems*; Bloor, D. M., Wyn-Jones, E., Eds.; Kluwer Academic Publishers: Netherlands, 1990; p 397; (b) Israelachvili, J. N.; Mitchell, D. J.; Ninham, B. W. *J. Chem. Soc., Faraday Trans. 2* **1976**, *72*, 1525. (c) Fogden, A.; Ninham, B. W. *Langmuir* **1991**, *7*, 590. (d) Hyde, S. T. *Pure Appl. Chem.* **1992**, *64*, 1617. (e) Israelachvili, J. N. In *Surfactants in Solution*; Plenum: New York, 1987; p 4. (f) Rosen, M. J. *Surfactants and Interfacial Phenomena*; John Wiley: New York, 1989; p 108.

(27) Evans, D. F.; Mitchell, D. J.; Ninham, B. W. *J. Phys. Chem.* **1984**, *88*, 6344.

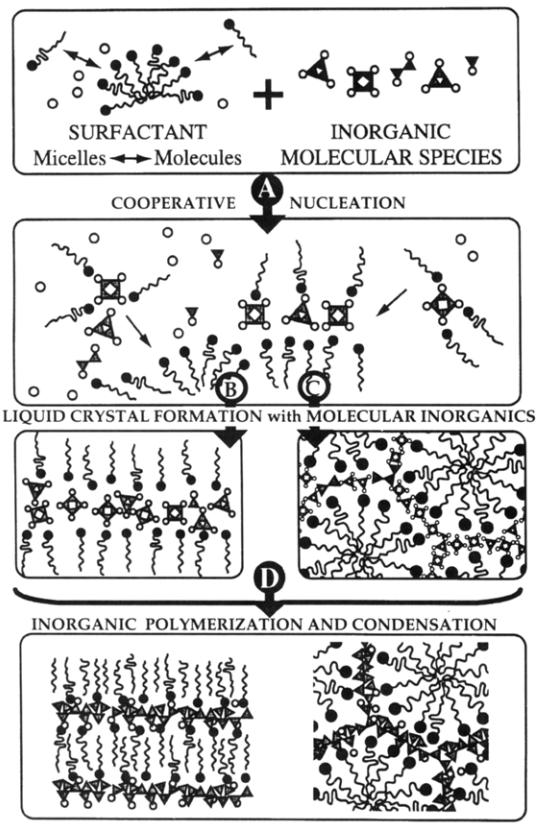

Figure 1. Cooperative templating model for biphase materials synthesis. (A) Single-chain surfactant molecules react preferentially with silicate polyanions (e.g. dimers, double three and four rings) which displace the original surfactants monoanions. Micelles serve as a surfactant molecule source or are rearranged according to the anion charge density and shape requirements. (B and C) Nucleation and rapid precipitation of organized arrays takes place with configurations determined by the cooperative interactions of ion-pair charges, geometries, and organic van der Waals forces. Silicate condensation at this stage at low temperatures is minimal. (D) Condensation of the silicate phase with increasing time and temperature. The silicate framework charge decreases during this process and may lead to liquid-crystal-like phase transitions as the surfactant phase tries to reorganize the changing interface charge density.

Fortunately there is considerable literature available to help evaluate the relative importance of $\Delta G_{org}(A,\rho_{org},...)$ in biphase materials synthesis. Information on the chemistry of soluble inorganic species is also available which is equally important. A brief review of some of the key aspects of surfactant and inorganic solution chemistry which provided the basis of the synthesis described in this paper follows.

Organic Species and Arrays. We have used a variety of surfactants, including cationic, anionic, two-tailed, with coupled head groups, fluorinated and zwitterionic species. Only the single-tailed cationic surfactants (C_nTMA) have been previously discussed in the context of periodic mesostructure synthesis, so that the following discussion concerns that class. For $C_{16}TMABr$ in water the micelle to hexagonal liquid-crystal phase transition is at about 28 wt %,[28] which is higher than that ordinarily used in silicate mesostructure synthesis. In this research surfactant concentrations which were too low for liquid-crystal phase formation in pure water solutions were used almost exclusively.

The organization of surfactant molecules into arrays at concentrations below the liquid crystal-phase region is characterized by the critical micelle concentration (cmc) which is denoted by the temperature and concentration at which finite organized ordered arrays can first be detected. At the lowest concentrations of surfactants at which micelle formation occurs the micelles are spherical or rodlike. With C_nTMA surfactants the spherical micelle forms first and then at higher concentrations may transform into a micelle with rodlike geometry as indicated in Figure 2. This is referred to as the second cmc (cmc2) since it is experimentally observed almost in the same fashion as the primary cmc (cmc1).[29] The sphere-to-rod transformation is strongly dependent on temperature, anion, and surfactant chain length (Figure 3).

At 70 °C the surfactant concentration has to be 25 wt % for the rodlike morphology to exist for $C_{16}TMABr$ (Figure 3a)[30,31] while at room temperature, ultrasonic,[31] ^{81}Br NMR,[32] light-scattering and viscosity measurements,[33] and ^{14}N NMR[34] studies show that the sphere to rodlike micelle transition is at 7–10 wt %. Neutron-scattering experiments show that the aspect ratio of the "rods" is ~2:1 for a 10 wt % solution of $C_{16}TMABr$.[35]

The stability of a micelle array and the sphere-to-rod transformation are also closely related to the degree of dissociation of the anion from the surfactant in the micelle array[36,37] (Figure 3b). For $C_{16}TMACl$ which has a relatively high degree of dissociation, a 40 wt % surfactant solution is required before the sphere-to-rod micelle transformation is obtained[29] at room temperature. $C_{16}TMAOH$ spherical micelles have low mean aggregation numbers, extensive polydispersity of micellar size and dissociation, and do not show the usual sharp break in conductivity associated with the existence of cmc1.[38] The rodlike geometry is even less stable for $C_{16}TMAOH$ than for $C_{16}TMACl$.

The rodlike micelle is also less favored for shorter surfactant chain lengths, and, for example, dodecyltrimethylammonium chloride ($C_{12}TMACl$) does not form rodlike micelles at any concentration.[39,40] The same can be said for the hydroxide, which as noted above, is even more highly ionized than the chloride. In view of (i) the fact that the hexagonal MCM-41 phases can be made at room temperature or higher using $C_{16}TMABr$, $C_{16}TMACl$, or $C_{16}TMAOH$ at surfactant concentrations as low as 1 wt % (with respect to water content)[3,41] well below cmc2, (ii) the ability to make hexagonal MCM-41 phases using short-chain surfactants such as $C_{12}TMAOH$ or $C_{12}TMACl$[14,15]

(28) Choudhury, S.; RoyYadav, R.; Maitra, A. N.; Jain, P. C. *Colloids Surf. A: Physicochem. Eng. Aspects*, **1994**, *82*, 49 and included references.

(29) Lindemuth, P. M.; Bertrand, G. L. *J. Phys. Chem.* **1993**, *97*, 7769.
(30) Reiss-Husson, F.; Luzzati, V. *J. Phys. Chem.* **1964**, *68*, 3504.
(31) Backlund, S.; Hoiland, H.; Kvammen, O. J.; Ljosland, E. *Acta Chem. Scand.* **1982**, *A36*, 698.
(32) Lindblom, G., Lindman, B.; Mandell, L. *J. Colloid Interface Sci.* **1973**, *42*, 400.
(33) Ekwall, P.; Mandell, L.; Solyom, P. *J. Colloid Interface Sci.* **1971**, *35*, 519.
(34) Henriksson, U.; Odberg, L.; Eriksson, J. C.; Westman, L. *J. Phys. Chem.* **1977**, *81*, 76.
(35) Quirion, F.; Magic, L. J. *J. Phys. Chem.* **1986**, *90*, 5435.
(36) Gamboa, C.; Rios, H.; Sepulveda, L. *J. Phys. Chem.* **1989**, *93*, 5540.
(37) (a) Biresaw, G.; McKenzie, D. C.; Bunton, C. A.; Nicoli, D. F. *J. Am. Chem. Soc.* **1985**, *89*, 5144. (b) Athanassakis, V.; Moffatt, J. R.; Bunton, C. A.; Dorshow, R. B.; Savelli, G.; Nicoli, D. F. *Chem. Phys. Lett.* **1985**, *115*, 467.
(38) Turq, P.; Drifford, M.; Hayoun, M.; Perera, A.; Tabony, J. *J. Phys. (Paris)* **1983**, *44*, L-471.
(39) Ozeki, S.; Ikeda, S. *Bull. Chem. Soc. Jpn.* **1981**, *54*, 552.
(40) Ikeda, S. *Colloid Polym. Sci.* **1991**, *269*, 49.
(41) Huo, Q.; Margolese, D.; Stucky, G. D., submitted to *J. Am. Chem. Soc.*

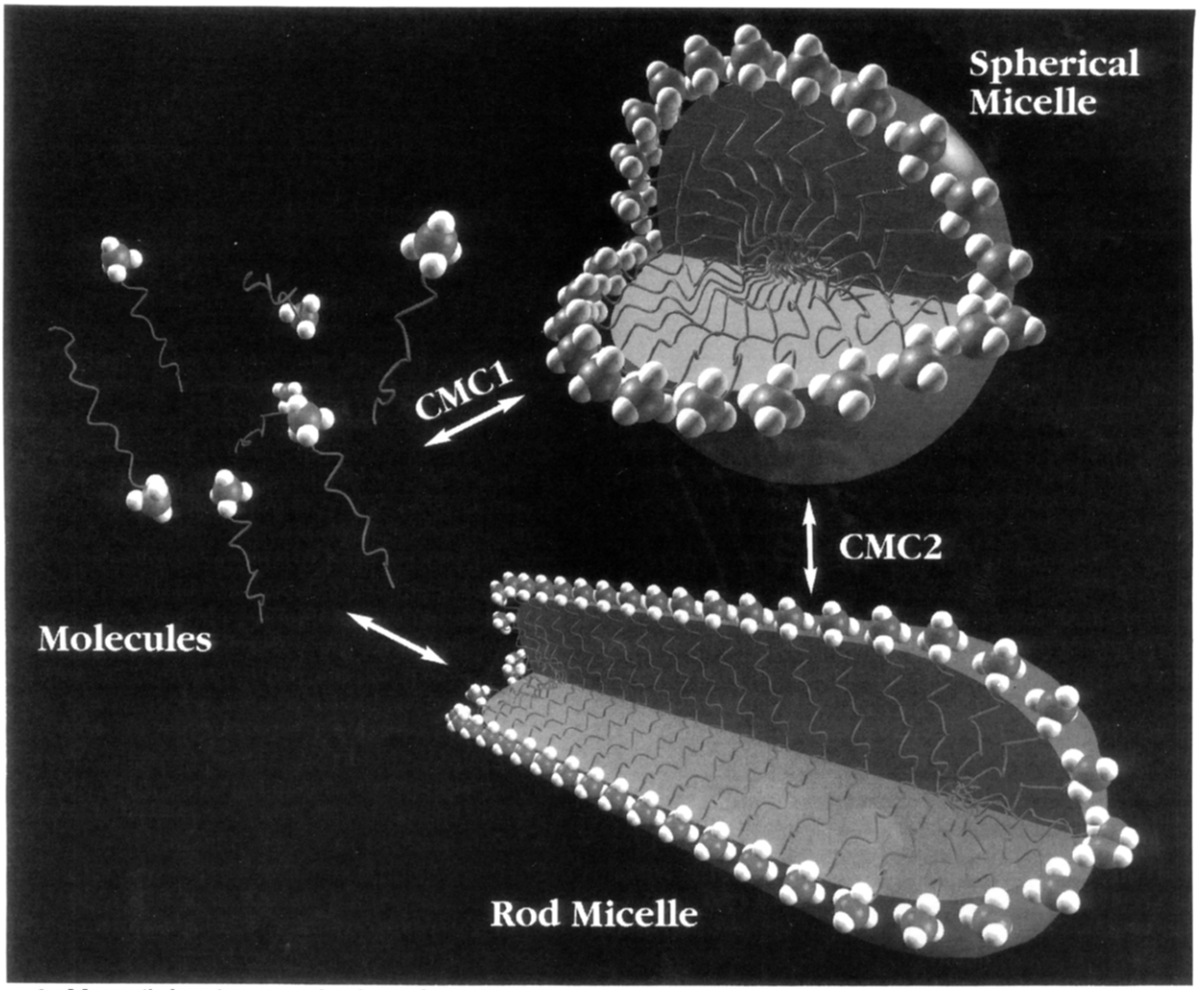

Figure 2. Monotailed surfactant molecules and micelles. The micelles are in dynamic equilibria with soluble molecular species. Critical micelle concentration 1 (cmc1) is the lowest concentration at which spherical micelle formation is observed. Cmc2 is the concentration at which the spherical to rodlike micelle transformation takes place.

for which there are no reported rodlike micelles in aqueous solutions, and (iii) the instability of rodlike micelles at temperatures above 70 °C where most of the reported syntheses of MCM-41 and MCM-48 have been carried out,[2,3,14,15,16,17] the presence of the preorganized rodlike micelles prior to adding the silicate phase does not appear to be a necessary factor in periodic biphase silicate synthesis. This has been further confirmed by *in situ* forced-flow small-angle neutron scattering measurements of the basic silicate mesostructure synthesis solutions.[18]

The spherical micelle geometry is clearly not a structure directing factor in the syntheses since the final lamellar, hexagonal, and cubic structures are not generated by spherical symmetry. Another consideration is that the kinetic instability of monotailed surfactant arrays has long been noted[42] and both spherical and rodlike micelles are in dynamic equilibrium with their monomers.[43] Anionic inorganic species therefore have ready access to soluble surfactant molecular species and can readily restructure micelle arrays.

We noted early in our studies that an important structure directing factor is the role of the highly charged anionic inorganic species which control the surfactant geometry through charge density matching and multidentate bonding.[2] An example in surfactant micelle chemistry is shown for $(C_{16}TMA)_2SO_4$ in Figure 3b.[44] The formation constant of an ion pair of a divalent anion with a cationic surfactant is generally higher than that for the monoanions (smaller degree of micelle dissociation). The divalent anion has a significant effect on surfactant organization and this is further evidence that polyionic inorganic molecular species might be used to control and define surfactant ordering and the ultimate biphase structure.

Molecular Inorganic Solution Species. Polydentate and polycharged molecular inorganic species that are present in solution[2,3,18] coordinate electrostatically with surfactant molecules which may originate from loosely structured micelles or unassociated organic molecules. In the case of basic (pH > 9.5) silicate syntheses, one can use the pK_a values reported by Iler[45] to establish the types of charged silicate molecular species which are present. The pK_a values of monomeric H_4SiO_4 and dimeric $H_2Si_2O_7$ are 9.5 and 10.7, respectively, and are partly (76 and 17%,

(42) The apparent microviscosities in the "interior" of aqueous micelles by ^{13}C NMR are ~8 cP (water = 1.0 cP, *n*-octanol = 8.9 cP, glycerol = 875 cP). Wong, M.; Thomas, J. K. In *Micellization, Solubilization and Microemulsions*, Mittal, K. L., Ed.; Plenum Press: New York, 1977; p 647.

(43) For example, see: Fendler, J. H. *J. Phys. Chem.* **1980**, *84*, 1485.

(44) Biresaw, G.; McKenzie, D. C.; Bunton, C. A.; Nicoli, D. F. *J. Am. Chem. Soc.* **1985**, *89*, 5144.

(45) Iler, R. K. *The Chemistry of Silica*; John Wiley: New York, 1979.

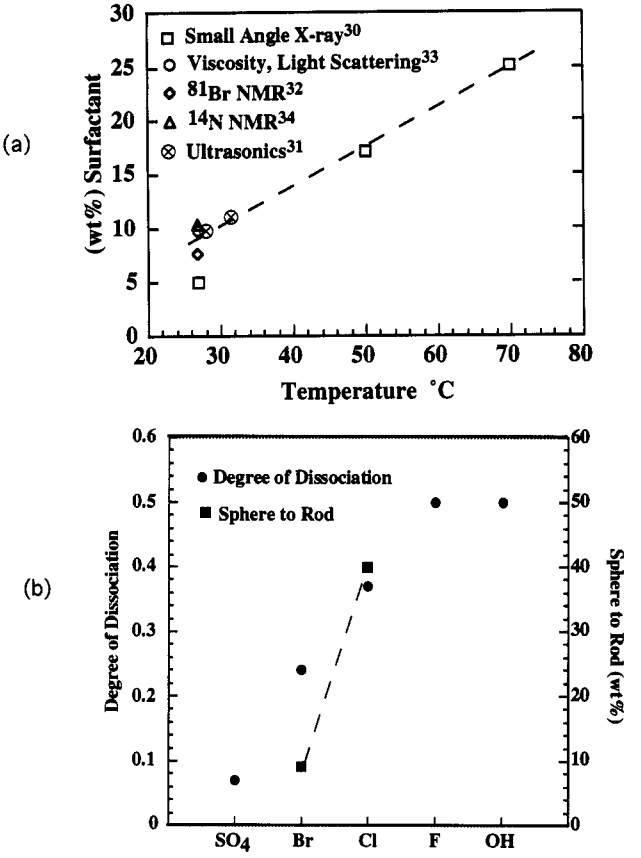

Figure 3. (a) Required weight percent of surfactant for the sphere-to-rodlike micelle transition of C_{16}TMABr as a function of temperature. (b) Degree of dissoziation of micelle arrays at room temperature of C_{16}TMAX for different types of anions. The greater the degree of dissociation is, the less stable the micelles are. This is reflected in the sphere to rodlike micelle transitions shown as a function of the required micelle concentration of cmc2 for C_{16}TMABr and C_{16}TMACl.

respectively) dissociated at a synthesis pH of ~ 10. Higher silicate oligomers (cyclic rings; double three, four, five or six rings) have pK_a values of about 6.5, and are therefore totally dissociated (> 99.9%) at pH ~ 10. It could be expected that the larger oligomers would therefore preferentially interact with the surfactant head groups. In the same manner that polycharged ions in micelle chemistry (see above) have a dramatic effect on the organic array configurations associated with monoanions and in general create new organic array morphologies,[18] polydentate inorganic ions in solution can be expected to be an important factor in determining organic array morphology through multidentate bonding and charge density matching of organic surfactant with the inorganic molecular species. The charge, geometry, and association of the molecular inorganic species in solution were adjusted through the use of pH, cosolvent, counterions, and temperature in the research reported in this paper.

The charge density of the inorganic species determines how many surfactant molecules are associated with a given inorganic molecular unit as well as the preferred orientation of the surfactant head group relative to the molecular inorganic species[46] (Figure 1A). This "charge density matching" determines the average intermolecular spacing between surfactant head groups and within that constraint and the energetics of the inter*molecular* interactions of the inorganic species, the molecular ion pairs adapt the preferred liquid crystal array morphology (Figure 1B,C). In its simplest kinetic form at low temperatures the synthesis is a three-stage process in which the first step can be viewed as the net ionic exchange of a polycharged anionic species (e.g., $[Si_8O_{20}H_x]^{x-8}$) for a monoanion (OH^-, Cl^-, Br^-, Figure 1A). These ion pairs can then organize into a new liquid-crystal-like array. The final step is condensation of the inorganic phase.

This model explains a number of interesting synthesis features of the basic (pH > 9.5) silicate MCM-41 synthesis. The room temperature synthesis space diagram[3] and the variation of product structure with pH and silica source[2] confirm that one can directly synthesize lamellar *or* hexagonal phases. Recent studies also show that cubic phases can be made at room temperature.[41]

With time and/or temperature silicate inorganic units condense (Figure 1D) and, not surprisingly, one can observe phase transformations,[2,41] i.e., if the synthesis for a poorly condensed lamellar phase is carried out in a synthesis region near the hexagonal phase, *in situ* NMR studies[47] show that subsequent condensation leads to a reduction of charge in the inorganic phase by the reaction

$$\equiv Si{-}O^- + HO{-}Si\equiv \rightarrow \equiv Si{-}O{-}Si\equiv + OH^- \quad (5)$$

or that condensation is also possible by the loss of solvent (water or ethanol) by the reaction

$$\equiv Si{-}OR + HO{-}Si\equiv \rightarrow \equiv Si{-}O{-}Si\equiv + ROH \quad (R = C_2H_5 \text{ or } H) \quad (6)$$

In the former cases, the reduced charge density per surface area of the inorganic gives a reconfiguration of the lamellar organic group surface into a surface with lower charge density/unit area, e.g., the hexagonal phase.[2,47]

Temperature Effects. The mechanism for biphase material synthesis is readily varied by adjusting the variables in eqs 1 and 3. At high temperatures (>50 °C) the kinetics of inorganic condensation dominate as ion-pair interactions and solvation effects become less important and hydrolysis rates increase. Enhancing these factors decreases the entropy associated with organic array formation, so that at higher temperatures both the thermodynamic ($\Delta G_{org}(A,\rho_{org},...)$) and kinetic favorability of organized organic arrays are reduced. An example of the consequences of this is the formation of zeolite phases (ZSM-35[48] and ZSM-48[49]) in syntheses above 150 °C.

In considering the application of the cooperative templating model previously proposed[2,3] and in order to evaluate the relative importance of the various kinetic terms in eq 3, we have chosen to use low temperature (5–50 °C) syntheses and molecular inorganic liquid-crystal routes.[18,47] At lower temperatures it is well established that silicate condensation is slow[50] under the reaction conditions used in ref 2. By using temperature dependent studies and particularly low temperatures, the formation

(46) Wiebcke, M.; Grube, M.; Koller, H.; Engelhardt, G.; Felsche, J. *Microporous Mater.* **1993**, *2*, 55.

(47) Bull, L.; Firouzi, A.; Kumar, D.; Oertli, A.; Stucky, G. D. and Chmelka, B. F. The 10th International Zeolite Conference; Germany, July, 1994.

(48) Jacob, N. E.; Joshi, P. N.; Shaikh, A. A.; Shiralkar, V. P. *Zeolites* **1993**, *13*, 430.

(49) Davis, M. E.; Chen, C.; Burkett, S. L.; Lobo, R. F. In *Better Ceramics Through Chemistry VI*, in press.

(50) Breck, D. W.; Flanigen, E. M. *Molecular Sieves*; Society of Chemical Industry: London, 1968; p 47.

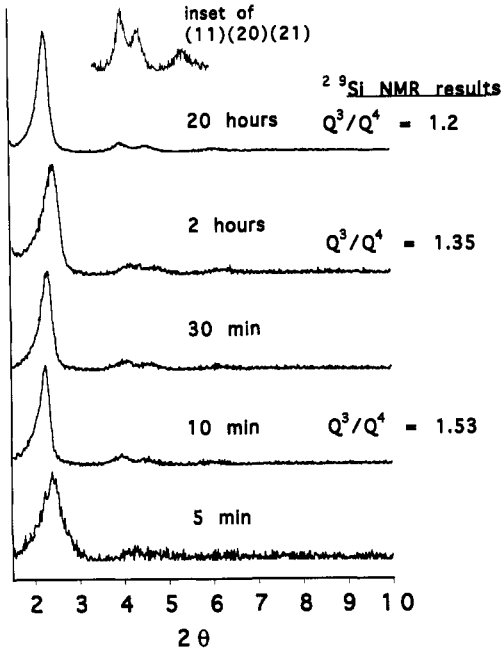

Figure 4. XRD patterns and ^{29}Si NMR results of the framework condensation of a hexagonal silicate mesophase synthesis with time. The XRD intensities are scaled to the (100) peak of the 20 h sample and for example the intensities of the 5 min sample are accordingly enhanced by a factor of 10. The experiments were prepared identically and varied only with respect to reaction time. 5.0 g of 2 mol L^{-1} NaOH was mixed with 2.8 g of C_{16}TMACl (25 wt %) and 38.0 g of water. To this solution 3.85 g of $Si(OC_2H_5)_4$ was added and the reaction allowed to proceed at room temperature.

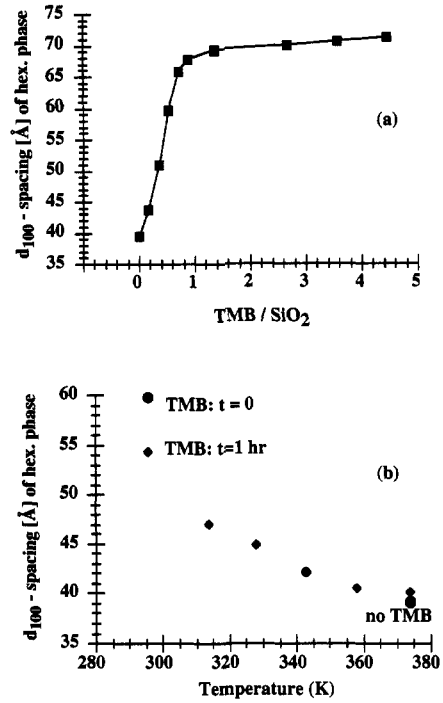

Figure 5. (a) Variation of the d_{100} spacing of the hexagonal phase as a function of the TMB/SiO_2 ratio (TMB = 1,3,5-trimethylbenzene). The chemical composition of the reaction mixture was $NaAlO_2$·5.3C_{16}TMACl·2.27TMAOH·15.9SiO_2·nTMB·1450H_2O. The products were obtained after refluxing for 5 h. (b) d_{100} spacing of the hexagonal phase as a function of time (t = 0 and 1 h at room temperature) and temperature of addition of TMB. The composition of the reaction mixture was the same as in Figure 5a (n = 8.5). The synthesis solution (without TMB) was preheated for one hour at the indicated temperature. The TMB was then added at that temperature, and then subsequently refluxed for 5 h (for the point labeled TMB: t = 0, TMB was added before preheating the synthesis solution).

of the structured organic array is more dominant[51] and its role in the biphase assembly process can be better differentiated from that of inorganic condensation and biphase interface interactions.

The room temperature silicate phases synthesized in basic media can be isolated as solids after short synthesis times. Already after 5 min the general features of the XRD pattern of a hexagonal phase are visible (Figure 4). The X-ray diffraction appearance time for a mesophase is strongly dependent on the silica source and can be made shorter than that in Figure 4 by using a soluble silicate. For example, a good hexagonal phase was obtained in 5 min by using sodium silicate solution N; and, the surfactant in this product could be readily removed by calcination at 500 °C. The samples associated with these very early stages show the characteristics of a salt, including dissolution when placed in distilled water. ^{29}Si MAS NMR results confirm for this preparation (using TEOS) the low degree of condensation of silicate at these early stages (Figure 4) and an increase in condensation with time.[47,52]

Solvent-templating effects, as evident in the role of water in liquid-crystal phases[53] or as shown by Beck et al.[14,15] in the use of "expanders" to control the pore size of the MCM-41 family, become increasingly important with decreasing temperature. Beck et al.[14,15] have demonstrated that the pore size of MCM-41 can be varied as a function of the concentration of expander molecules such as 1,3,5-trimethylbenzene (TMB). Following the methodology introduced by Beck et al., we also observed using C_{16}TMACl and TMB that this expansion of the pore size can be done only by introducing the expander (TMB) at low temperatures and/or short reaction times *before* significant silicate condensation takes place (see Figure 5). The alkylated aromatic expander "dissolves" in the organic hydrophobic tail (see Figure 6) of the surfactant (or vice versa, depending on concentration). The hydrophobic solvation interaction of the aromatic molecules with the hydrocarbon tails is analogous to the hydrophilic solvation interaction of water with the charged head groups in concentrated liquid crystal C_nTMA$^+$X$^-$ (X$^-$ = OH$^-$, Cl$^-$, etc.) arrays. In this sense the inorganic/organic molecular ion pair species are organized with the organic TMB molecules as a *cosolvent* for the hydrophobic portion of the biphase synthesis mixture. The addition of other organic solvents in the synthesis of porous materials could be used to provide further structure directing possibilities.

Synthesis Approach: Molecular Inorganics and Surfactants. These and other results[47] strongly suggest that a general *molecular inorganic* liquid-crystal approach to mesostructure synthesis using low temperatures and mild synthesis conditions might be successful with other compositions. The cooperative organization of ion pairs formed between inorganic molecular species in solution and surfactant molecules is determined at low temperatures by both electrostatic interactions and hydrophobic van der Waals forces. The usual chemistry of liquid-crystal

(51) Auvray, X.; Petipas, C.; Anthore, R.; Rico, I.; Lattes, A. *J. Phys. Chem.* **1989**, *93*, 7458.

(52) The degree of condensation depends on the synthesis parameters, including particularly pH source of silica, temperature, and surfactant. Larger degrees of condensation have been observed for the hexagonal and lamellar phases using other conditions.

(53) Tiddy, G. J. T. *Phys. Rep.* **1980**, *57*, 1.

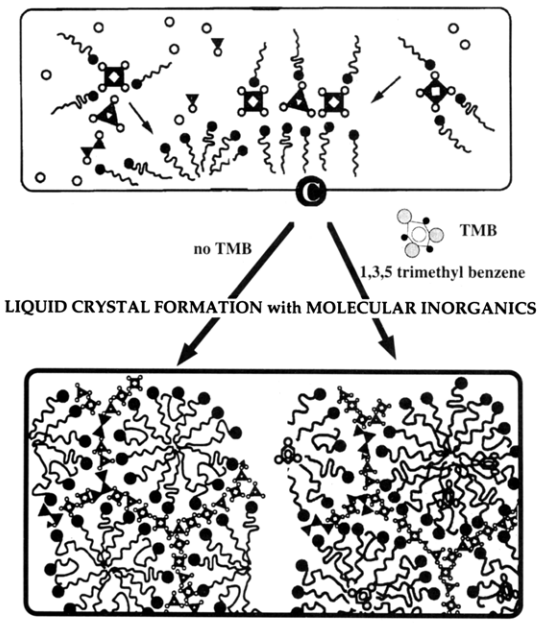

Figure 6. Cosolvent, pore expansion, and wall thickness.

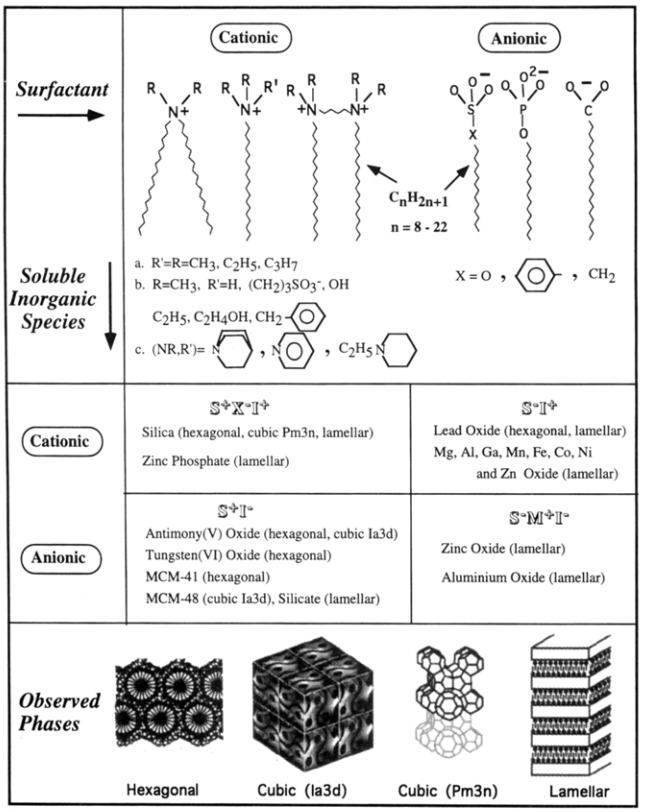

Figure 7. General scheme for the syntheses pathways by combination of different surfactant and soluble inorganic species.

arrays created by using charged surfactants applies under these conditions. For example, if a biphase interface is generated with a high charge density and with the appropriate surfactant structure, low curvature surfaces with small organic head-group areas will be generated.[26] In this way by initially adjusting the charge density matching, surfactant geometry and relative reactant concentrations, the various mesostructure geometries can be generated.

We classify four general pathways[19] to the synthesis of mesostructured surfactant–inorganic biphase arrays as outlined in Figure 7. The first route involves the interaction of anionic inorganic solution species with cationic surfactants (S^+I^-), which we have discussed in detail above; the syntheses of MCM-41 and MCM-48[2,3,14–17] are prototypic examples. Following the model described above, we describe how the scope of this route can be extended to non-silica-based systems. A similar route but involving the cooperative condensation of a cationic inorganic solution species with an anionic surfactant (S^-I^+) to give hexagonal mesostructures is demonstrated for the first time. These possibilities had already been predicted,[2] although no examples were known at that time. By contrast, routes 3 and 4 are novel in that assembly of ionic inorganic species proceeds in the presence of similarly charged surfactants, but mediated by small ions of opposite charge or bonded to the surfactant molecules, i.e., small anions for cationic surfactants with cationic solution species ($S^+X^-I^+$) ($X^- = Cl^-, Br^-$), or with reversed charges for all ions ($S^-M^+I^-$) ($M^+ = Na^+, K^+$). Since most results were obtained for routes 1 and 3, and route 3 is a novel process, the further discussion will concentrate on these two systems with the focus on pathway 3: the formation of silica mesophases under extremely acidic conditions.

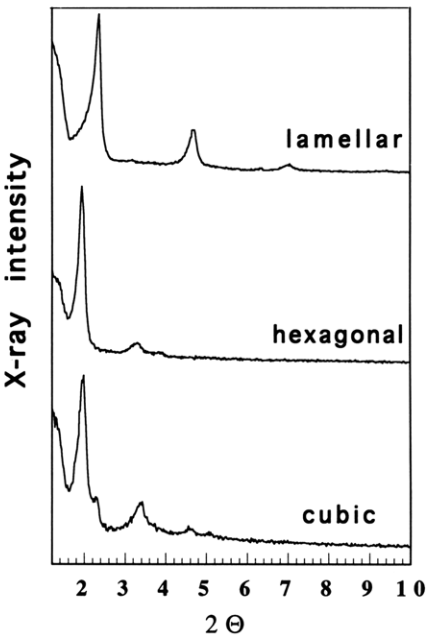

Figure 8. Powder X-ray diffraction (XRD) patterns of mesostructured antimony(V) oxide materials.

I. Combination of S^+I^-: Syntheses of Tungsten(VI) and Antimony(V) Oxide Mesophases. Lamellar, MCM-41 and MCM-48 periodic porous silicates (S^+I^-) are obtained under basic conditions by the cooperative organization of *anionic* solution silicate species and *cationic* surfactant molecules.[2,3,14,15,16,17,54] Such a mechanism[2] is expected to work for other oxides as well, if the pH, counterions and solvent are chosen appropriately to adjust the geometry and charge density of the metal oxide polyanions in solution balanced against surfactant charge and packing requirements. Thus, we were able to synthesize a lamellar tungsten oxide (d_{100} = 28.3 Å) at pH above 9, and a mixture of the lamellar and a hexagonal phase (d_{100} = 40 Å) at pH 4–8 using cationic surfactants, as demonstrated by X-ray diffraction and TEM.[19]

Another example for this synthesis route is the formation of a cubic (*Ia3d*, a = 105(3) Å), hexagonal (d_{100} = 46 Å)

(54) Inagaki, S.; Fukushima, Y.; Kuroda, K. *J. Chem. Soc., Chem. Commun.* **1993**, 680.

and lamellar (d_{100} = 37.5 Å) antimony(V) oxide mesophase in the pH range 6.0–7.0 (see Figure 8). Depending on the antimony/surfactant ratio of the starting mixture and the pH, which is adjusted by adding slowly a diluted HBr solution to the clear starting mixture of pH = 7, three different mesophases could be synthesized. Decreasing the pH of the starting mixture with a $[Sb(OH)_6]^-/C_{18}H_{37}(CH_3)_3N^+$ ratio of 10:1 to pH 6.7–6.8 resulted in the cubic antimony oxide mesophase, while lowering the pH further (6.2–6.5) led to the hexagonal phase. With a $[Sb(OH)_6]^-/C_{18}H_{37}(CH_3)_3N^+$ ratio of 5:1 only the lamellar mesophase is formed in the pH range 6.0–7.0. Below pH = 6 only amorphous material was obtained. The appearance of structurally similar mesophases at lower pH compared to the silicate is to be expected, since the tungsten and antimony isopoly acids are more acidic than the silicic acid. Cooperative biphase templating can thus be carried out at neutral and lower pH values by matching the charge density of the oxide solution molecular species to that of the respective surfactant phase.

Investigations to calcine these mesoporous materials are still in progress. So far, we can say that the calcination process which works for the silica mesophases (heating the samples first in pure nitrogen and then in pure oxygen with slow heating rates of 1 K min^{-1} up to 550 °C) has not led to tungsten and antimony oxide mesostructured materials. The framework of these materials collapsed during this calcination process probably due to a reduction of the framework either by a redox process with the template (for the tungsten oxide materials) or an intrinsic instability of the higher oxidation state (for the antimony(V) oxide materials) at high temperatures. At the moment we are examining more gentle chemical and physical ways to remove the surfactants from the mesostructured materials without destroying the framework.

II. Combination of S^-I^+: Formation of Metal Oxide Mesophases. A similar approach was undertaken in a situation in which the ionicity of the components was reversed and an *anionic* surfactant was used to direct the condensation of *cationic* oxide species (S^-I^+, see Table 1). $C_{16}H_{33}SO_3H$ was used in the synthesis of Fe and Pb oxide mesostructured materials. Hexagonal (d_{100} = 45.8 Å) and lamellar (29.2 Å) Pb oxide phases could be obtained, while in the case of iron oxide mixtures of different lamellar phases were isolated.[55] Using soluble precursors of Mg, Al, Ga, Mn, Fe, Co, Ni, and Zn oxides in combination with $C_{12}H_{25}OPO_3H_2$ mostly lamellar phases are formed. Fe^{2+}, Fe^{3+}, Ni^{2+}, Co^{2+}, or Mn^{2+} solutions combined with sodium alkyl sulfates ($C_nH_{2n+1}OSO_3Na$ with n = 12, 14, 16, 18) at room temperature lead to lamellar phases (see Table 1). Starting with $C_{12}H_{25}OSO_3Na$ and $C_{14}H_{29}OSO_3Na$ surfactants as precursors, thermal analysis of the pure product samples revealed that the final products were hydrated salt-like materials of the alkyl sulfate surfactants and the transition metals with a composition of $(C_nH_{2n+1}OSO_3^-)_2M^{2+}\cdot nH_2O$ or $(C_nH_{2n+1}OSO_3^-)_2M_2O_2^{2+}\cdot nH_2O$ (for M = Fe^{3+}). For comparison, longer chain surfactants such as $C_{16}H_{33}OSO_3Na$ and $C_{18}H_{37}OSO_3Na$ yield materials with a higher degree of condensation among the transition metal ions. The latter characteristically have significantly lower surfactant contents in the products. In some cases mixtures of different lamellar phases are obtained, as indicated by the presences of more than one set of (h00) Bragg peaks (Table 1). Another interesting example of this S^-I^+ composite system is aluminum oxide with sodium dodecylbenzene-sulfonate at 70 °C and pH = 3.5 which slowly rearranges to increase the layer spacing (from 28.9(0.8) Å after 8 h to 32.1(0.8) Å after 9 days). The surfactant head group is presumably a part of the inorganic framework in this group.

Table 1. Typical Synthesis Results Using Different Inorganic Precursor and Surfactants

inorganic precursor	surfactant	phase	highest XRD peak d spacing (Å)
antimony oxide	$C_{18}H_{37}(CH_3)_3NBr$	cubic (*Ia*3*d*)	42.9
antimony oxide	$C_{18}H_{37}(CH_3)_3NBr$	hexagonal	46.0
antimony oxide	$C_{18}H_{37}(CH_3)_3NBr$	lamellar	37.5
tungsten oxide	$C_{16}H_{33}(CH_3)_3NBr$	hexagonal	40.0
tungsten oxide	$C_{16}H_{33}(CH_3)_3NBr$	lamellar	28.3
zinc phosphate	$C_{10}H_{21}(CH_3)_3NBr$	lamellar	21.6
zinc phosphate	$C_{12}H_{25}(CH_3)_3NBr$	lamellar	23.5
zinc phosphate	$C_{14}H_{29}(CH_3)_3NBr$	lamellar	26.0
zinc phosphate	$C_{16}H_{33}(CH_3)_3NBr$	lamellar	28.2
zinc phosphate	$C_{18}H_{37}(CH_3)_3NBr$	lamellar	30.5
zinc phosphate	$C_{20}H_{41}(CH_3)_3NBr$	lamellar	32.5
alumina	$C_{12}H_{25}C_6H_4SO_3Na$	lamellar	28.9
Pb^{2+}	$C_{16}H_{33}SO_3H$	hexagonal	45.8
Pb^{2+}	$C_{16}H_{33}SO_3H$	lamellar	38.5
Fe^{2+}	$C_{16}H_{33}SO_3H$	lamellar	41.0
Mg^{2+}	$C_{12}H_{25}OPO_3H_2$	lamellar	31.0
Mn^{2+}	$C_{12}H_{25}OPO_3H_2$	lamellar	28.6
Fe^{3+}	$C_{12}H_{25}OPO_3H_2$	lamellar	26.9
Co^{2+}	$C_{12}H_{25}OPO_3H_2$	lamellar	30.8
Ni^{2+}	$C_{12}H_{25}OPO_3H_2$	lamellar	31.1
Zn^{2+}	$C_{12}H_{25}OPO_3H_2$	lamellar	29.6
Al^{3+}	$C_{12}H_{25}OPO_3H_2$	lamellar	26.4
Ga^{3+}	$C_{12}H_{25}OPO_3H_2$	lamellar	27.2
Fe^{2+}	$C_{12}H_{25}OSO_3Na$	lamellar	21.0
Fe^{2+}	$C_{14}H_{29}OSO_3Na$	lamellar	23.0
Fe^{2+}	$C_{16}H_{33}OSO_3Na$	lamellar	27.3
Fe^{2+}	$C_{18}H_{37}OSO_3Na$	lamellar	30.3
Fe^{3+}	$C_{12}H_{25}OSO_3Na$	lamellar	23.1
Fe^{3+}	$C_{14}H_{29}OSO_3Na$	lamellar	26.0
Fe^{3+}	$C_{16}H_3OSO_3Na$	lamellar	28.1
Fe^{3+}	$C_{18}H_{37}OSO_3Na$	lamellar	31.0
Co^{2+}	$C_{12}H_{25}OSO_3Na$	lamellar	20.9 and 39.7
Co^{2+}	$C_{14}H_{29}OSO_3Na$	lamellar	22.8
Co^{2+}	$C_{16}H_{33}OSO_3Na$	lamellar	41.5 and 27.4
Co^{2+}	$C_{18}H_{37}OSO_3Na$	lamellar	28.4
Ni^{2+}	$C_{14}H_{29}OSO_3Na$	lamellar	31.8, 23.5, 23.2
Ni^{2+}	$C_{16}H_{33}OSO_3Na$	lamellar	43.5 and 27.5
Ni^{2+}	$C_{18}H_{37}OSO_3Na$	lamellar	24.3
Mn^{2+}	$C_{14}H_{29}OSO_3Na$	lamellar	23.3
Mn^{2+}	$C_{16}H_{33}OSO_3Na$	lamellar	42.2 and 28.9
Mn^{2+}	$C_{18}H_{37}OSO_3Na$	lamellar	24.3
tin sulfide	$C_{16}H_{33}(CH_3)_3NBr$	lamellar	25.8

III. Combination of $S^+X^-I^+$: *Syntheses of silica mesophases*: Surprisingly, the formation of silica mesophases is also possible by the cooperative assembly of *cationic* inorganic species with *cationic* surfactants. For example, silica mesophases can be formed using a combination of cationic surfactant (S^+), halogen anion (X^-), and cationic silicic acid species (I^+). Figure 9 shows the XRD patterns of the as-synthesized mesophases. Table 2 shows the typical synthesis results. The use of alkyltrimethylammonium ($C_nH_{2n+1}(CH_3)_3N^+$, n = 10, 12, 14, 16, 18) resulted in the formation of hexagonal phases. Large head-group surfactants (such as alkyltriethylammonium $C_nH_{2n+1}(C_2H_5)_3N^+$, n = 12, 14, 16, 18) favored the cubic *Pm*3*n* phase. Long-chain ($C_nH_{2n+1}(CH_3)_3N^+$, n = 20, 22) or bichain (dialkyldimethylammonium) surfactants led to the formation of lamellar phases. High-quality samples of the three phases can be formed over a wide range of strongly acidic conditions (1–7 mol L^{-1} HCl or HBr). We found that HCl favors the formation of all three phases,

(55) Ciesla, U.; Demuth, D.; Leon, R.; Petroff, P.; Stucky, G.; Unger, K.; Schüth, F. *J. Chem. Soc., Chem. Commun.* **1994**, 1387.

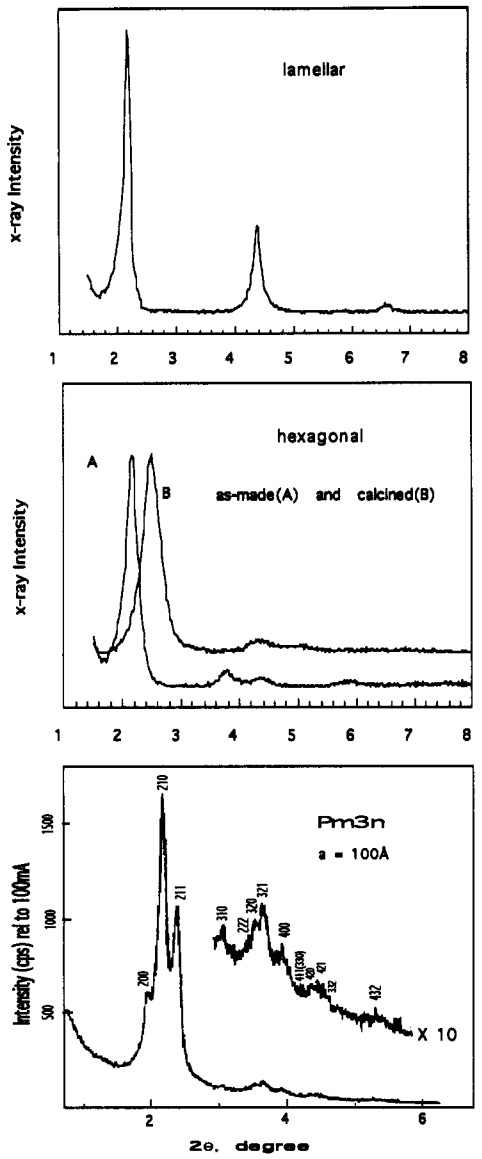

Figure 9. XRD patterns of as-made and calcined silica mesostructures precipitated from acidic medium. The patterns of the lamellar and hexagonal phase were collected on a Scintag PADX diffractometer, the pattern of the cubic phase (*Pm3n*) was measured at the synchrotron X-ray source at Brookhaven National Laboratory using a wavelength of λ = 1.7048 Å.

while HBr favors the formation of the hexagonal and not the *Pm3n* phase, even using cetyltripropylammonium, with its large head group, as the template. One factor driving the formation of the hexagonal phase and eliminating the cubic phase when using HBr is that the bromide ion is a strongly binding counterion[56] which reduces the effective head group area of the surfactant below A_{min} for globular micelles.[26] Other acids (HF, $HOOCCH_3$, H_2SO_4, H_3PO_4, and HNO_3) in the same range of $[H^+]$ concentration produced amorphous solids or transparent gels within 2 h.

In contrast to the synthesis conditions used previously[2,3,14,15] for M41S silicate mesophases, a concentrated acidic medium, low-temperature, short synthesis times and low concentrations of surfactant were employed. Some surfactants other than alkyltrimethylammonium ions were also good templates for the acid syntheses of mesoporous material; e.g., alkyldimethylamine, zwitterionic, and dimeric quaternary ammonium surfactants where the first two are protonated under the synthesis conditions. Silica polymerization proceeds through the condensation of cationic intermediates in this pH range and results in gel and glass morphologies which are strikingly different from those produced using basic pH.[45,57] The new large-cage (~30 Å) cubic (*Pm3n*) silica phase and the hexagonal and lamellar silica mesostructures are the first examples of cationic silica solution species leading to periodic porous materials but, more importantly, in conjunction with the cooperative templating model[19] define a strategy for the general synthesis of mesostructured materials using combinations of cationic (S^+) or anionic (S^-) surfactants and anionic (I^-) or cationic (I^+) inorganic soluble precursors.

Table 2. Typical Synthesis Results of Silica Mesophase from Acidic Medium

surfactant R	composition (mole) R	HX	$(C_2H_5O)_4Si$	H_2O	product phase
$C_{15}H_{33}N(CH_3)_2$	0.12	4.9 HCl	1.0	130	hexagonal
$C_{18}H_{37}N(CH_3)_2$-$[(CH_2)_3SO_3]$	0.12	5.0 HCl	1.0	130	hexagonal
16–10–16[a]	0.06	4.9 HCl	1.0	130	hexagonal
$C_{16}H_{33}N(CH_3)_3^+$	0.12	9.2 HCl	1.0	130	hexagonal
$C_{16}H_{33}N(CH_3)_3^+$	0.12	4.9 HBr	1.0	130	hexagonal
$C_{16}H_{33}N(C_3H_7)_3^+$	0.12	4.9 HBr	1.0	130	hexagonal
$C_{16}H_{33}N(C_2H_5)_3^+$	0.13	10.4 HCl	1.0	130	cubic (*Pm3n*)
$C_{16}H_{33}N(C_2H_5)$-$(C_5H_{10})^+$[b]	0.13	10.4 HCl	1.0	130	cubic (*Pm3n*)
$C_{20}H_{41}N(CH_3)_3^+$	0.12	4.9 HCl	1.0	130	lamellar
$(C_{12}H_{25})_2N(CH_3)_2^+$	0.12	6.2 HCl	1.0	150	lamellar

[a] 16–10–16 = $[C_mH_{2m+1}(CH_3)_2N$–C_sH_{2s}–$N(CH_3)_2C_mH_{2m+1}]Br_2$ (m = 16, s = 10). [b] $C_{16}H_{33}N(C_2H_5)(C_5H_{10})^+$ = cetylethylpiperidinium.

Lamellar $ZnPO_4$ synthesis: Using a similar synthetic approach and excess H_3PO_4 (pH ~2.5), lamellar C_nH_{2n+1}-$(CH_3)_3N^+X^-[HZnPO_4]$ (n = 10, 12, 14, 16, 18, 20; X = Cl^-, Br^-) phases can be formed from solutions containing $[H_2ZnPO_4]^+$. In one of these phases, there is three-dimensional ordering and excellent registry between the inorganic layers which are separated by up to 32.5 Å for n = 20. At least four different lamellar phases (spacings 28.2, 29.7, 37.3, and 63 Å) with different d spacings and surfactant packing, including monolayer and bilayer geometries, can be generated by controlling composition and pH. This approach can be applied to different framework compositions. One of them can be formed from solutions containing $[H_2ZnPO_4]^+$ (pH ~2.5) and like the acid silica phases contains one halide ion per surfactant molecule. For example, $[C_{16}H_{33}N(CH_3)_3^+Br^-]\cdot HZnPO_4$ (d_{001} = 28.2 Å), observed and calculated components are respectively Zn (12.35%, 12.45%), Br (15.41%, 15.23%), N (2.89%, 2.67%), and P (5.53%, 5.90%). Its XRD peaks (Figure 10) could be indexed on an orthorhombic cell having a = 6.49 Å, b = 6.57 Å, and c = 28.08 Å. An STA run in air showed organic loss with decomposition between 220 and 450 °C. The black residue at 900 °C (69% loss; calculated 71) gave a diffraction pattern of only $Zn_2P_2O_7$.

IV. Combination of $S^-M^+I^-$ Zincate and Aluminate Layer Syntheses. The synthesis of mesophases is also possible by a fourth pathway using a cation to mediate the anionic charges of the surfactant and inorganic solution species. For instance, $Zn(OH)^{3-}$, $Zn(OH)_4^{2-}$, and $Zn_2(OH)_6^{2-}$

(56) Bleasdale, T. A.; Tiddy, G. J. T.; Wyn-Jones, E. *J. Phys. Chem.* **1991**, *95*, 5385.

(57) Brinker, C. J.; Scherer, G. W. *Sol-Gel Science*; Academic Press: San Diego, 1990.

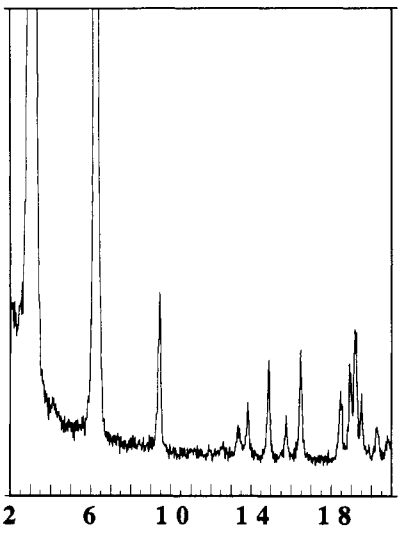

Figure 10. XRD pattern of lamellar zinc phosphate mesophase (produced using $C_{16}H_{33}(CH_3)_3NBr$).

are the predominant species of a 0.1 mol L^{-1} solution of ZnO (pH = 10–14).[58] The anionic surfactant $CH_3(CH_2)_{16}COO^-M^+$ gives a lamellar zinc oxide phase (d_{100} = 48.8 and 50.3 Å; $M^+ = Na^+$ and K^+, respectively) about pH = 12.5 ($(CH_3)_4NOH$ without surfactant under the same reaction conditions gives only ZnO), suggesting a mediated templating ($S^-M^+I^-$) pathway. Like the silica mesophases synthesized under acidic conditions this is an example of the organic phase indirectly interfaced with the inorganic phase via an intermediate cation. Anionic surfactants compete with oxide/hydroxide groups for coordination sites and under the same conditions phosphates such as $C_{12}H_{25}OPO_3Na_{2-x}H_x$ (x = 0–1) appear to coordinate directly to the zinc atom, thus becoming part of the framework with no sodium ions present in the final product.

Other interesting examples are the alumina-based phases. At pH > 8, an anionic aluminate species in solution resulted in the formation of a lamellar phase: $[C_{12}H_{25}OPO_3NaH]_3{\cdot}Al(OH)_3{\cdot}7.5H_2O$, observed and calculated components Al (2.5%, 2.49%), P (8.55%, 8.56%), C (40.17%, 40.1%), H (7.7%, 7.5%), and Na (5.56%, 6.35%). Another lamellar phase, $[C_{12}H_{25}OPO_3]{\cdot}Al(OH){\cdot}H_2O$, observed and calculated components Al (7.90%, 8.28%), P (9.27%, 9.50%), C (44.36%, 44.17%), H (8.55%, 8.59%), was formed at pH <5. The d spacing of the former (33.6 Å) is bigger than that of the latter (27.5 Å, see Figure 11). The former is consistent with a ($S^-M^+I^-$) solution pathway and no framework phosphate, while in the latter the (S^-I^+) chemistry prevails with surfactant framework participation.

In addition to chemical analysis and to the difference in d spacing providing evidence for the two synthetic pathways, ^{31}P MAS NMR provides support for S^-I^+ and $S^-M^+I^-$ via the chemical shift of the two materials. As can be seen in Figure 12 the material made at pH > 8 has a peak between –2 and –5 ppm and the material made at pH < 5 shows a peak at –11 ppm. Following the ^{31}P NMR assignments of Mortlock et al.[59] and Akitt et al.[60] a soluble species of Al complexed to $H_2PO_4^-$ ligands $[Al(H_2PO_4)]^{2+}$ with the Al bridged to the P atom via an oxygen atom has a ^{31}P peak between –9 and –11 ppm. This peak corresponds to the chemical shift range found for the layered aluminophosphates made at pH < 5, indicating the presence of a bridging oxygen between the Al and the P according to the S^-I^+ mechanism. For a soluble species containing an Al complexed to H-bonded polymeric phosphorus ligands the chemical shift range is in the region –3 to –6 ppm. This corresponds to the chemical shift range for the material made in the pH > 8 region which contains surfactant hydrogen bonded to the aluminate framework. Due to charge balance the Na cations as part of the interface between surfactant and inorganic material are probably coordinated to the phosphate head groups of the surfactant molecules.

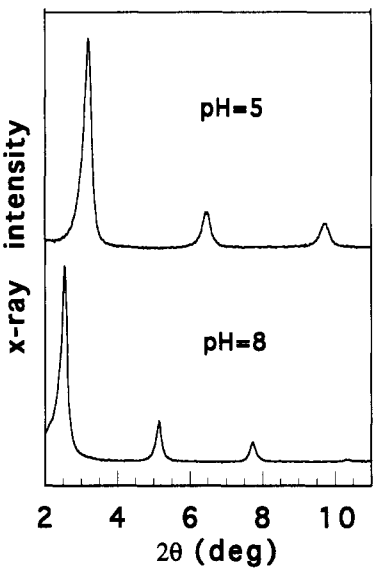

Figure 11. XRD patterns of lamellar alumina phases (using $C_{12}H_{25}OPO_3^-$ as template) obtained at different pH's.

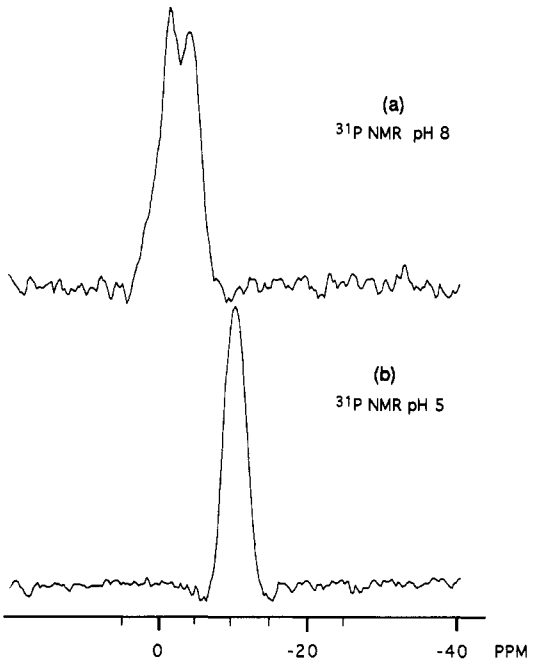

Figure 12. ^{31}P MAS NMR of alumina-containing alkyl phosphate surfactant. (a) $[C_{12}H_{25}OPO_3NaH]_3{\cdot}Al(OH)_3{\cdot}7.5H_2O$ synthesized at pH > 8. (b) $[C_{12}H_{25}OPO_3]{\cdot}Al(OH){\cdot}H_2O$, synthesized at pH < 5.

(58) Baes, Jr. C. F.; Mesmer R. E. *The Hydrolysis of Cations*; Wiley-International Publication: New York, 1976; p 287.
(59) Mortlock, R. F.; Bell, A. T.; Radke, C. J. *J. Phys. Chem.* **1993**, *97*, 767.
(60) Akitt, J. W.; Greenwood, N. N.; Lester, G. D. *J. Chem. Soc. A* **1971**, 2450.

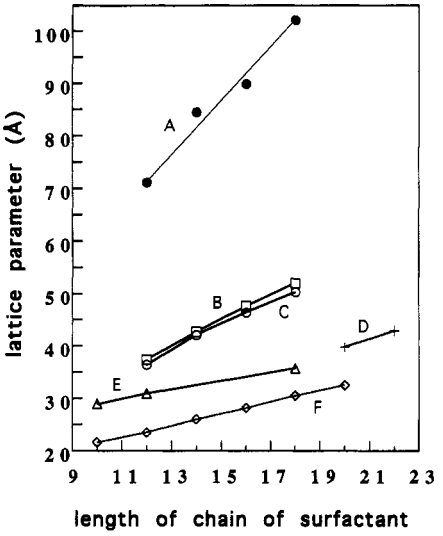

Figure 13. The relationship between unit cell parameter and number of carbon atoms in the surfactant chain. (A) Cubic silica (*Pm3n*) phase using alkyltriethylammonium. Hexagonal silica and silicate phases using alkyltrimethylammonium from acidic (B) and basic (C) media, respectively. Lamellar silica phases using $C_nH_{2n+1}(CH_3)_3N^+$ with n = 20, 22 (D) and dialkyldimethylammonium (E) in acidic medium. Lamellar $ZnPO_4$ (F) using alkyltrimethylammonium.

The surfactant hydrocarbon chain has no effect on the chemical shift of the ^{31}P atom. This circumstance allows for a direct comparison with the NMR assignments of Mortlock et al.[59] and Akitt et al.[60] for the above materials. To establish this, ^{31}P MAS NMR spectra of the surfactant used in the layered alumina $C_{12}H_{25}OPO_3H_2$ (DDP) and its sodium salt $C_{12}H_{25}OPO_3NaH$ (DDP-Na^+) were collected. DDP showed a signal at approximately 0 ppm corresponding to the H_3PO_4 standard. The head group of DDP is similar to H_3PO_4 with one of the H atoms replaced by a $C_{12}H_{25}$ alkyl chain. Its sodium form showed a signal with a ^{31}P chemical shift at 4 ppm corresponding to the chemical shift of phosphates.[59]

The structure of the materials was also investigated by ^{27}Al MAS NMR. Both materials showed resonance signals with chemical shifts between 5 ppm and −20 ppm relative to $Al(NO_3)_3$ in aqueous solution indicating that all the Al is octahedrally coordinated.[61]

Characterization of $S^+X^-I^+$ Silica Mesostructure Materials. The as-made surfactant–silica mesophases exhibit different unit-cell parameters when surfactants with differing alkyl chain lengths are used (Figure 13). For the as-synthesized hexagonal product (using $C_{16}H_{33}(CH_3)_3N^+$), STA and chemical analysis gave (wt %) SiO_2, 39.7; $C_{16}H_{33}(CH_3)_3N^+$, 46.38; Cl^-, 5.75. The surfactant/Cl ratio in the product is therefore 1.0:1.0 (the lamellar product containing $C_{20}H_{41}(CH_3)_3N^+$ gave the same ratio), a feature that distinguishes these mesostructure phases from the M41S family, which have no significant halide content using the same surfactant halide starting materials. Well-formed polyhedral crystals with dimensions on the order of 10–20 μm were typically found for this hexagonal phase.

Since in the acid mesophase product the surfactant cationic charge is exactly balanced by a chloride anion, the surfactant should be removable without providing an exchangeable cation as required for the anionic framework of MCM-41.[62] It was found that more than 85% of the surfactant could be removed from the as-synthesized material by stirring it in pure ethanol at room temperature or by overnight reflux. The removal of the surfactant was also possible by calcination. A lattice contraction of about 7 Å was observed upon calcination (Figure 9). The calcined hexagonal phases (at 500 °C) had surface areas greater than 1000 m^2/g and average pore diameters of 18.6, 26.5, and 33.2 Å for $C_{14}H_{29}(CH_3)_3N^+$, $C_{16}H_{33}(CH_3)_3N^+$, and $C_{18}H_{37}(CH_3)_3N^+$, respectively, as determined by N_2 BET measurements.

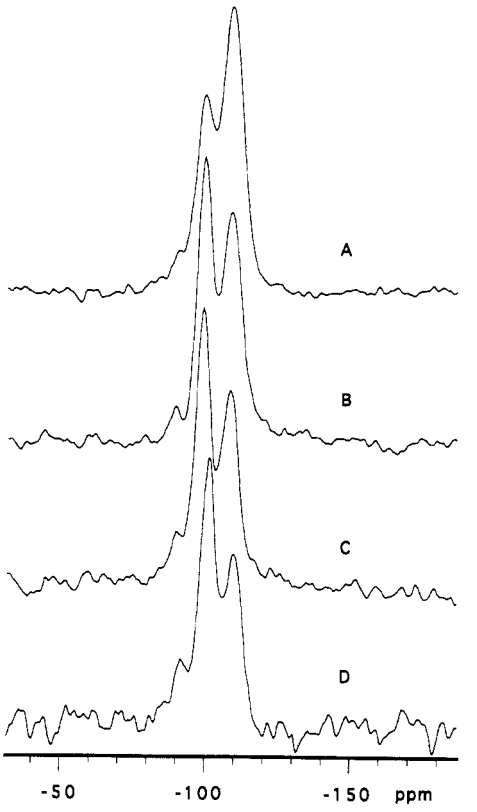

Figure 14. ^{29}Si MAS NMR of silica mesophases. (A) hexagonal (longer reaction time, 2 h, Q^3/Q^4 = 0.59), (B) cubic (*Pm3n*, Q^3/Q^4 = 1.1), (C) hexagonal (normal reaction time, 0.5 h, Q^3/Q^4 = 1.1), and (D) lamellar (Q^3/Q^4 = 1.4).

The XRD data (Figure 13) show that similar surfactants at pH < 0 produce mesostructures with similar, but apparently slightly larger, d spacings than those obtained by synthesis in a basic medium. For example, $C_{18}H_{37}(CH_3)_3N^+$ in this paper shows a d_{100} spacing of 45.0 (0.8) Å, while a d_{100} spacing of 43.6 (0.7) Å was found in highly basic medium (pH 12–13). The silica wall structure may not be the same in strong acid as opposed to strong base syntheses; however, one would expect that the ($S^+X^-I^+$)-mediated configuration would result in a slightly larger d spacing for the same surfactant than for the direct (S^+I^+) configuration obtained in basic synthesis.

The new cubic silica phase was prepared using surfactants with larger head groups (for example, alkyltriethylammonium, cetylethylpiperidinium). This was done to decrease the value of the surfactant packing parameter in order to generate maximum surface curvature.[26,56] The XRD data closely match (intensities and indexing) those for the I_1 (*Pm3n*) cubic phase of cetyltrimethylammonium

(61) Wu, Y.; Chmelka, B. F.; Pines, A.; Davis, M. E.; Grobet, P. J.; Jacobs, P. A. *Nature* **1990**, *346*, 550.

(62) Whitehurst, D. D. U.S. Patent, 5,143,879, 1992.

chloride and cetylpyridinium chloride in formamide.[63] This cubic phase consists of a packing of two types of discrete micellar aggregates[63,64,65,66,67] in globular-like cages, with one large cage of ~30 Å giving a clathrasil-like structure. Upon calcination (at 500 °C) to remove the template, the cell edge shrinks, e.g., from 89.9 to 78.2 Å for the sample containing $C_{16}H_{33}(C_2H_5)_3N^+$ and 102.2 to 83.8 Å for $C_{18}H_{37}(C_2H_5)_3N^+$. This silica mesophase is an example of a mesostructured material with large cages and a high concentration of silanol groups in the framework as determined by ^{29}Si NMR spectroscopy (see Figure 14).

^{29}Si MAS NMR data (Figure 14), were used to determine the degree of polymerization and the concentration of silanol groups, as measured by the ratio Q^3/Q^4. All the spectra of the materials in this figure show the two major peaks Q^3 (−101 to −102 ppm) and Q^4 (−110 to −111 ppm).[68] From the areas of the Q^3 and Q^4 signals the number of ^{29}Si of the type $(SiO)_3{\equiv}\mathit{Si}{-}OH$ and $(SiO)_3{\equiv}\mathit{Si}{-}O{-}Si{\equiv}$ could be determined, respectively. The estimated error in the values of Q^3 and Q^4 are about ±5% of their value. Hexagonal phase A is a sample synthesized at short reaction time (30 min) while the hexagonal phase B was reacted under the same synthesis conditions except for the longer reaction time of 2 h. The Q^3/Q^4 ratio measures the extent of silanol group condensation, indicating for material B a more condensed framework than for material A. Q^3/Q^4 for the hexagonal phase and for the lamellar phase in acidic media after long reaction times are similar to those corresponding products found for materials precipitated from basic media (0.55 and 1.2, respectively) using either higher temperature synthesis or long reaction times.

Figure 15 illustrates the STA results for the as-synthesized silica mesophases. These samples show similar decomposition behavior with three distinct stages of weight loss: for example, for the cubic *Pm3n* phase containing $C_{16}H_{33}(C_2H_5)_3N^+$ (Figure 15c), a first step up to 140 °C, a second one between 140 and 425 °C, and finally a third from 425 to 640 °C are clearly visible in the diagram. The first endothermic weight loss is due to the desorption of water. The second one, exothermic in nature, indicates the combustion and decomposition of the organic surfactant in air. Being initially fast and then slowing, this step suggests that different decomposition products are produced during the calcination of the surfactant. The third stage is related to water losses via condensation of silanol groups to form siloxane bonds and continuing loss of residual hydrocarbon. Above 640 °C, a few remaining silanol groups in the framework continue to polymerize resulting in a very small weight loss of about 1%. The as-synthesized samples contained more than 50 wt % organic species.

Silica Mesophase Formation Mechanism under Acidic Conditions. As in the case of the basic condensation process[2,3,14-17] where the formation of MCM-41 is explained by the condensation of oligomeric silicate molecular species coordinating to cationic surfactant

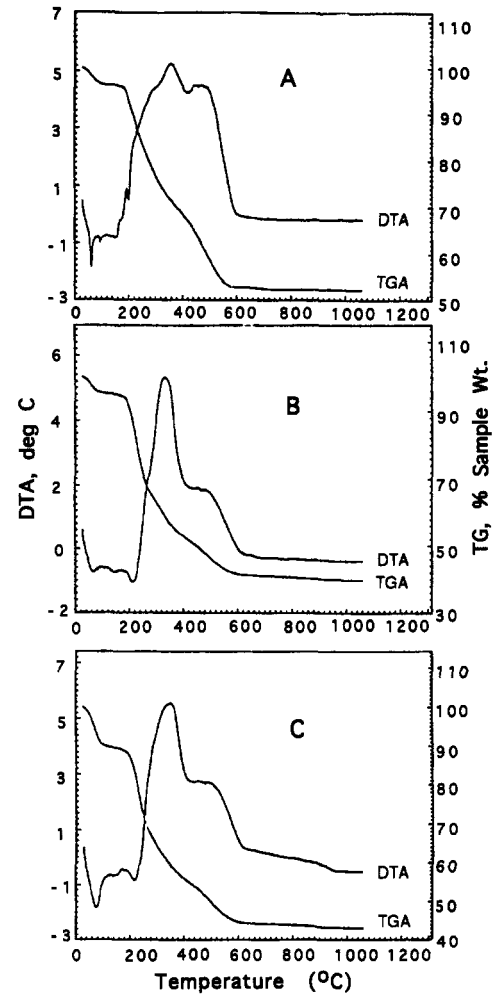

Figure 15. STA of silica mesophases. (A) lamellar (containing $C_{20}H_{41}(CH_3)_3N^+$), (B) hexagonal (containing $C_{16}H_{33}(CH_3)_3N^+$), and (C) cubic *Pm3n* (containing $C_{16}H_{33}(C_2H_5)_3N^+$) phases.

molecules, we believe that the main driving force for self-assembly at low pH is electrostatic interface energy, including hydrogen bonding ($\Delta G_{inter}(A,\rho_{inorg},\rho_{org},...)$). At high concentrations of hydrohalogen solutions, the cationic hydrophilic region of the surfactant is surrounded by halide ions forming an electrical double layer with a peripheral negative charge (S^+X^-). Silica sources (such as TEOS, $SiCl_4$) hydrolyze at this pH to silicic acid and positively charged oligomeric intermediates. The alkoxide and silanol groups are easily protonated, for example to $\equiv Si(OH_2)^+$,[57] in the extremely acidic medium. The positively charged silica species (I^+) are attracted electrostatically to the anionic portion of the surfactant ion pair (S^+X^-) forming an electrical triple layer ($S^+X^-I^+$), where the halide (X^-) ions coordinate through Coulombic interactions to the protonated silanol groups. We suggest that the cationic silica and halide-cationic micellar interactions are the dominant force for initiating the self-assembly process in the concentrated acidic medium.

During the cooperative assembly of the soluble molecular species in the concentrated acid silica synthesis, precipitation and some polymerization proceeds. In this process the protons associated with the silica species, along with associated excess halide ions, are excluded until a neutral inorganic framework remains. The surfactant cation and X^- (1:1) are probably associated with the neutral polysilicic acid (silica containing silanol) framework through $\equiv Si{-}OH{\cdots}X^-S^+$ linkages. The H^+ concentration, ac-

(63) Auvray, X.; Abiyaala, M.; Duval, P.; Peptipas, C.; Rico, I.; Lattes, A. *Langmuir* **1993**, *9*, 444.
(64) Vargas, R.; Mariani, P.; Gulik, A.; Luzzati, V. *J. Mol. Biol.* **1992**, *225*, 137.
(65) Charvolin, J.; Sadoc, J. F. *J. Phys. (France)* **1988**, *49*, 521.
(66) Seddon, J. M.; Templer, R. H. *Philos. Trans. R. Soc. London, A* **1993**, *344*, 377.
(67) Fontell, K. *Colloid Polym. Sci.* **1990**, *268*, 264.
(68) Lippma, E.; Magi, M.; Samoson, A.; Engelhardt, G.; Grimmer, A. R. *J. Am. Chem. Soc.* **1980**, *102*, 4889.

cording to the mechanism, should be the same before and after the synthesis, as was observed experimentally.

This mediated ($S^+X^-I^+$) model is supported by the following evidence: (i) the cationic silica species which are present at pH < 2 (refs 45 and 57) and the fact that H^+ concentration in the solution does not change during synthesis; (ii) the 1:1 surfactant to chlorine ratio in the hexagonal and lamellar products; (iii) the easy removal of the surfactant with ethanol; (iv) the observation that TEOS and $SiCl_4$ hydrolyze and form mesophase products while Cab-O-Sil (SiO_2) which does not readily hydrolyze in acidic conditions, forms no mesophase products; and (v) the anion dependence of the synthesis, e.g., the different products obtained with Cl^-, Br^-, and oxyanions.

It is clear that the mechanism for ($S^+X^-I^+$) synthesis is not the same as that for (S^+I^-) synthesis. This is not surprising in view of the marked differences in silica sol–gel chemistry under acidic and basic conditions and the fact that the extension of molecular sieve silicate syntheses from the usual basic pH to strongly acidic pH conditions has not been previously achieved. This is therefore the first reported example of periodic porous silica syntheses at a pH < 2.

The lamellar $C_nH_{2n+1}(CH_3)_3N^+X^-[HZnPO_4]^+$ with n = 10, 12, 14, 16, 18, 20; X = Cl^-, Br^- mesophases, with structures which we believe are analogous to the previously determined structures of layered $MH(ZnPO_4)_2$ (M = Na, Cs)[69] structures, strongly support a ($S^+X^-I^+$) model similar to that for the acid synthesized silica phases, with the cationic surfactant indirectly coordinated to the $HZnPO_4$ walls via hydrogen bonding to the anion.

Summary

The syntheses described above were based on low-temperature conditions, charged inorganic molecular species and pH controlled inorganic condensation. Polycharged inorganic species tend to displace the surfactant monoanions, reduce the concentration of free surfactant molecules which were at equilibrium with the original micelles and induce a reorganization of the organic surfactant molecules. The charge density of the molecular inorganic species thus initially determines the interface packing density and the resulting biphase geometry of the surfactant molecules by the number of surfactant molecules that can coordinate to a given soluble inorganic species and the surfactant orientations which are favored relative to the inorganic species.

The cooperative rearrangement of these new ion pairs is determined at low temperatures by both electrostatic interactions and the hydrocarbon tail van der Waals forces. The usual chemistry of liquid-crystal arrays using charged surfactants applies at this point. If the generated biphase interface has a high charge density, low-curvature surfaces with small organic head-group areas will be formed. More specifically, the overall topology of the composite mesostructure is determined in a local molecular sense by the dimensionless effective surfactant packing parameter, $g = V/lA_0$,[26] and the collective surface bending energy[70] as proscribed by the inorganic species charge density. By initial adjustment of the charge density matching, surfactant geometry, and relative reactant concentrations, various mesostructure geometries can be generated, usually with incomplete inorganic condensation.

The products obtained for the acid silica mesophase syntheses are cubic ($Pm3n$), hexagonal, and lamellar phases with increasing value of g, respectively. The initial cooperative templating process does not require a precursor liquid-crystal surfactant phase or even an isotropic micelle phase. The ultimate topology of the composite mesostructure is a reflection of the liquid-crystal-like assembly of the molecular inorganic/surfactant ion pairs so that regardless of the inorganic composition, liquid-crystal morphologies have been observed and can be expected.[18,47]

Since the inorganic polymerization or condensation is not a requirement for mesostructure formation, this chemistry provides an excellent route for the use of molecular cluster precursors for the subsequent synthesis of extended inorganic condensed phases. This can be done by selected inorganic polymerization procedures using pH and temperature, or by introducing ions which bridge the molecular units as covalent or coordination linkages through the addition of agents such as sulfide, or by electrochemical control of inorganic oxidation states.

The versatility of the cooperative templating chemistry, which is relevant to the synthesis of these new composite materials, offers many possibilities. We have demonstrated the feasibility of using the synergistic interface chemistry, of inorganic and organic species to create periodic mesostructures with (i) cationic or anionic inorganic species, (ii) main-group or transition-metal oxides, and (iii) cationic or anionic surfactants. The surfactants may be anionic or quaternary ammonium salts, and can be two-tailed lipid-like, dimeric, with large head groups or zwitterionic. Each surfactant can be used in a lyotropic sense, giving rise to one or more structural phases depending on concentrations, cosolvents, and temperature among other variables. In addition to the four different types of mesophases synthesized so far (hexagonal, cubic ($Ia3d$ and $Pm3n$) and lamellar), the other known liquid crystal bi- and tricontinuous geometries should be accessible. While the inorganic frameworks in the examples presented here are silicate, silica, main-group and transition-metal oxides, sulfides, and phosphate; other inorganic compositions are also undoubtedly feasible.

The variety of surfactants which were used, including anionic, lipid, and zwitterionic types makes this chemistry directly applicable to biomimetics and should provide an important pathway to biorelated materials. The chemistry emphasized in this paper applies when the conditions in eqs 3 and 4 are satisfied. With two-tailed surfactants, ΔG_{org} is smaller than for monotailed surfactants and the preorganized biomimetic organic array approach, e.g., the deposition of bulk phase silica[10] or iron oxide[12] on organic tubules, becomes more important as the conditions contributing to organic array stability described in eq 2 are satisfied. A biomineralization analogy is metal oxide/hydroxide cluster assembly within the very strongly bound organic framework of apoferritin.[71]

We suggest that more generally Nature uses a global approach in biomineralization with varying degrees of cooperative structure direction by *both* the organic and inorganic components to create the intricate microscale morphologies found in biosilicates, such as diatoms or in

(69) Nenoff, T. M.; Harrison, W. T. A.; Gier, T. E.; Calabrese, J. C.; Stucky, G. D. *J. Solid State Chem.* **1993**, *107*, 285.
(70) Gruner, S. M. *J. Phys. Chem.* **1989**, *93*, 7562.
(71) Mann, S.; Wade, V.; Treffry, A.; Yewdall, S. J.; Harrison, P. M.; Levi, S.; Arosio, P. *Int. Congr. Ser.-Excerpta Med.* 1002 (Chemistry and Biology of Mineralization **1992**, Tissue); p 399.

calcium carbonate shell growth in gastropods and sea urchin spines.[72] The dynamic relationship between organic and inorganic phases makes possible (i) growth transitions and metamorphosis, (ii) the development of distinct functional units, and (iii) the integration of different inorganic structural phases into a biphase composite arrangement as determined by the biogenic requirements of the organism.

The periodic biphasic arrays described above can also have complicated bicontinuous and even potentially tricontinuous structures. By using the low temperature molecular building block synthesis described above,[2,3] more elaborate and inorganic-rich phases can be constructed[73] using the molecular surfactant/inorganic cluster "salts" as precursors. The work presented here made use of temporal and spatial control of the relative rates of the biphase and interface assembly processes in cooperative templating, and there is every reason to believe that this same approach can be used to impose microscopic long-range modulation of the periodic composite array morphology in a manner directly relevant to biomaterial synthesis.[74,75]

Acknowledgment. The suggestions and comments of Rosa Leon, Pierre M. Petroff, and Jacob Israelachvili, Joe Zasadzinski (UCSB), and Stephen Mann (University of Bath) are gratefully acknowledged. Funds were provided by the Office of Naval Research (G.D.S., P.S., and D.I.M.), NSF Grant DMR 92-08511 (G.D.S., D.G.D., and Q.H.), Air Products (G.D.S., T.E.G., and Q.H.), the NSF NYI program (B.F.C.), the Camille and Henry Dreyfus Foundation (BFC), the David and Lucile Packard Foundation (B.F.C.), and the DFG (P.S., U.C., D.G.D. and F.S. (Schu 744/6-1)). This work made use of MRL Central Facilities supported by the National Science Foundation under Award No. DMR-9123048.

(72) Inoue, S.; Okazaki, K. *Sci. Am.* **1977**, *236*, 83.
(73) Sieger, P.; et al., manuscript in preparation.
(74) Friedbacher, G.; Hansma, P. K.; Ramli, E.; Stucky, G. D. *Science* **1991**, *253*, 1261.
(75) Morse, D. E.; Cariolou, M. A.; Stucky, G. D.; Hansma, P. *Mater. Res. Soc. Symp. Proc.* **1993**, *292*, 59.